Universidade de Aveiro Departamento de Química
2008

Carla Andreia Cunha Vilela

Síntese e Caracterização de Nanocompósitos de Celulose/$CaCO_3$

Synthesis and Characterization of Cellulose/$CaCO_3$ Nanocomposites

Universidade de Aveiro Departamento de Química
2008

Carla Andreia Cunha Vilela

Síntese e Caracterização de Nanocompósitos de Celulose/$CaCO_3$

Synthesis and Characterization of Cellulose/$CaCO_3$ Nanocomposites

dissertação apresentada à Universidade de Aveiro para cumprimento dos requisitos necessários à obtenção do grau de Mestre em Ciência e Engenharia de Materiais, realizada sob a orientação científica do Doutor Carlos de Pascoal Neto, Professor Catedrático do Departamento de Química da Universidade de Aveiro e do Doutor Tito da Silva Trindade, Professor Associado do Departamento de Química da Universidade de Aveiro

o júri

presidente

Doutor João Carlos Matias Celestino Gomes da Rocha
Professor Catedrático da Universidade de Aveiro

Doutor Carlos de Pascoal Neto
Professor Catedrático da Universidade de Aveiro

Doutora Verónica Cortés de Zea Bermudez
Professora Associada com Agregação da Universidade de Trás-os-Montes e Alto Douro

Doutor Tito da Silva Trindade
Professor Associado da Universidade de Aveiro

agradecimentos

Em primeiro lugar gostaria de agradecer ao meu orientador, Professor Doutor Carlos Neto, por me ter proporcionado a oportunidade de desenvolver este trabalho, pela valiosa orientação científica, pelo incentivo e disponibilidade constantes.

Agradeço também ao Prof. Doutor Tito Trindade, co-orientador desta dissertação, pela disponibilidade e proveitosas contribuições no decurso deste trabalho.

O meu profundo agradecimento à Doutora Carmen Freire pela forma incansável e generosa como disponibilizou o seu tempo e conhecimentos para me acompanhar na realização deste trabalho, pela leitura de revisão desta dissertação, pelas oportunas correcções e sugestões e pela ajuda inexcedível e dedicada sem a qual as dificuldades científicas teriam sido muito mais difíceis de superar.

Aos professores da 2ªedição do Mestrado Europeu em Ciência e Engenharia de Materiais (EMMS) gostaria de manifestar a minha gratidão pela excelente equipa de docência e por todos os ensinamentos transmitidos.

Aos meus colegas e amigos de laboratório: Ana Marques, Ana Oliveira, Ana Sofia Santiago, Andreia Sousa, Dora Coelho, Fabiane Oliveira, Gil Gonçalves, Gisela Cunha, Paula Marques, Paula Pinto, Ricardo Pinto, Rui Domingues, Sandra Magina, Sara Lisboa, Sónia Santos e Susana Fernandes, gostaria de agradecer pelo apoio pessoal e pelo bom ambiente constante.

Ao Prof. Pedro Fardim e colaboradores (Åbo Akademi University, Turku, Finlândia) agradeço as análises de ToF-SIMS e XPS, bem como a disponibilidade e ajuda na interpretação dos respectivos resultados.

Agradeço a todos os membros do Departamento de Química que de alguma forma contribuíram para este trabalho.

À Comissão Europeia agradeço pelo apoio financeiro no âmbito do Projecto Europeu SUSTAINPACK IP-500311-2: Síntese e Caracterização de Novos Materiais com Base em Fibras de Celulose, por uma bolsa de técnico de investigação para realização do trabalho experimental.

Os últimos são também os primeiros a quem agradeço o apoio incondicional, o amor e a alegria de partilhar o dia-a-dia: à minha mãe, ao meu pai, ao meu irmão e ao meu “maridão”!

palavras-chave

Nanocompósitos, fibras de celulose, partículas de carbonato de cálcio, polietileno

resumo

Nanocompósitos de celulose/$CaCO_3$ foram preparados através da reacção controlada em meio alcalino entre cloreto de cálcio e carbonato de dimetilo na presença de fibras de celulose. O efeito de vários parâmetros reaccionais (tempo e temperatura de reacção, quantidade de fibra, e conteúdo de grupos carboxilo na celulose) nas características dos nanocompósitos foi avaliado por ICP-AES, IR, XRD, SEM, TGA, ToF-SIMS e XPS. Os resultados indicam que as condições de hidrólise influenciam a quantidade e morfologia das partículas de $CaCO_3$ depositadas na surperfície das fibras de celulose: (i) a quantidade e o tamanho das partículas de $CaCO_3$ depositadas nas fibras de celulose aumentam com o tempo de reacção; (ii) reacções realizadas a 25ºC originam nanopartículas esféricas de $CaCO_3$, enquanto que a 70ºC originam micro-agregados de $Ca(OH)_2$; (iii) suspensões de fibra de baixa consistência favorecem a formação de partículas esféricas; (iv) a presença de grupos carboxilo na celulose promove o crescimento controlado do $CaCO_3$ à superfície das fibras.

Compósitos de matriz polimérica de polietileno são uma possível aplicação para os nanocompósitos de celulose/$CaCO_3$. O uso dos nanocompósitos como fase de reforço originou materiais compósitos com maior módulo de armazenamento do que o polietileno. Para além disto, o valor do módulo de armazenamento dos compósitos de PE reforçados com celulose/$CaCO_3$ é superior ao módulo dos compósitos de PE reforçados só com fibras de celulose.

keywords Nanocomposites, cellulose fibres, calcium carbonate particles, polyethylene

abstract

Nanocomposite materials of cellulose/$CaCO_3$ were prepared by the controlled reaction between calcium chloride and dimethylcarbonate in alkaline medium in the presence of cellulosic fibres. The effect of several reaction parameters (reaction time, temperature, fibre quantity and extent of cellulose modification) on the final characteristics of the nanocomposite materials was investigated by ICP-AES, IR, XRD, SEM, TGA, ToF-SIMS and XPS. The results showed that the hydrolysis conditions strongly influenced the quantity and morphology of $CaCO_3$ particles deposited on the surface of cellulosic fibres: (i) the amount and size of $CaCO_3$ deposited on the cellulose fibres increased with increasing reaction time; (ii) the reactions performed at 25ºC originated nanosized $CaCO_3$ particles with spheroid morphology, while at 70ºC micrometric aggregates of $Ca(OH)_2$ were obtained; (iii) lower consistencies of the reacting suspensions favoured the formation of spheroidal particles; (iv) the presence of carboxyl groups at the cellulose surface promoted the selective control growth of $CaCO_3$ on the surface of the fibres.

Polymer matrix composites of polyethylene were a potential application for the nanocomposites of cellulose/$CaCO_3$. The use of the nanocomposites as reinforcing phase originated composite materials with higher storage modulus than neat PE. Besides, the modulus of PE composites reinforced with cellulose/$CaCO_3$ materials was even higher than the corresponding modulus of PE composites reinforced with only cellulose fibres.

CONTENTS

ABBREVIATIONS

ACC	Amorphous Calcium Carbonate
AKD	Alkyl Ketene Dimer
ATR	Attenuated Total Reflectance
BC	Bacterial Cellulose
CC	Carboxyl Content
CMC	Carboxymethylcellulose
DMA	Dynamic Mechanical Analysis
DMC	Dimethylcarbonate
DP	Degree of Polymerization
DS	Degree of Substitution
DSC	Differential Scanning Calorimetry
E'	Storage Modulus
ECF	Elemental Chlorine Free
FTIR	Fourier Transform Infrared Spectroscopy
ΔH_m	Melting Enthalpy
ΔH_0	Melting Enthalpy for 100% crystalline polymer
HDPE	High Density Polyethylene
ICP-AES	Inductively Coupled Plasma-Atomic Emission Spectrometry
IR	Infrared Spectroscopy
LDPE	Low Density Polyethylene
MCAA	Monochloroacetic Acid
ML	Middle Lamella
NaCMC	Sodium Carboxymethylcellulose
P	Primary Wall
PAM	Polyacrylamide
PCC	Precipitated Calcium Carbonate
PCN	Polymer-Clay Nanocomposites
PE	Polyethylene
PE-g-MA	Polyethylene-graft-Maleic Anhydride
PEI	Polyethylenimine
PEO	Poly(ethylene oxide)
PLA	Poly(lactic acid)

PMDI	Polymethylene diphenyl diisocyanate
PVdE-HFP	Poly(vinylidene fluoride hexafluopropylene)
S	Secondary Wall
S1	Thin Outer Layer
S2	Thick Middle Layer
S3	Thin Inner Layer
SEM	Scanning Electron Microscopy
TGA	Thermogravimetric Analysis
ToF-SIMS	Time-of-Flight Secondary Ion Mass Spectrometry
T_m	Melting temperature
W	Warty Layer
Xc	Crystalline fraction
XRD	X-Ray Diffraction
XPS	X-Ray Photoelectron Spectroscopy

LIST OF FIGURES

LIST OF TABLES

INTRODUCTION

Cellulose is an almost inexhaustible polymeric raw material with outstanding properties [1]. This polysaccharide has been for many years an important raw material used in the form of intact wood for construction purposes, natural textile fibres (cotton), or paper and board. The use of cellulose as a chemical raw material started in the 19th century with the production of the first cellulose derivative (cellulose nitrate) and the corresponding technical synthesis of "celluloid", the first thermoplastic polymer [1]. After this, cellulose began to be chemically transformed into a wide range of stable derivatives to be used in domestic life and several areas of industry [2].

Cellulose and its derivatives are promising raw materials to be applied in the field of composites. The growing interest of scientists for composites over the past few decades was triggered by the great potential of these materials for high added-value applications [3,4]. The stimulus of this interest is related with the enormous versatility of the synthetic processes and the almost endless choices of feasible combinations that can be employed to obtain composite structures [5]. Cellulose and cellulose derivatives have either been used as matrices or reinforcement materials in composites, though the majority of the research done so far dealt with cellulosic fibre reinforced polymeric composites [3-6]. Cellulose has been used in organic/inorganic composites in combination, for instance, with silica [7,8], titanium dioxide [9], gold [10], and kaolin particles [11], among others. The most widespread example of a man-made composite material is paper which is formed by cellulose fibres and mineral additive particles like $CaCO_3$, kaolin and TiO_2. Bearing this in mind, several authors [8-12] have reported that cellulosic fibres can be efficient hydrophilic substrates in the nucleation and growth of inorganic particles in aqueous medium, allowing the production of cellulose-based micro- and nanocomposites with great potential applications.

Calcium carbonate is one of the most abundant biominerals formed by living organisms (corals, pearls, mollusc shells, egg shells and the exoskeleton of arthropods). At an industrial level, besides its application in papermaking, $CaCO_3$ has been mainly used as a filler in composite

materials such as in plastics or as a pigment in paints and in paper coating dispersions. Therefore the ability to manufacture $CaCO_3$ with specific morphology, structure, and particle size might have important consequences for future developments in these industries [13].

The information regarding composite materials of calcium carbonate and cellulose is very scarce since only few studies dealt with cellulose/$CaCO_3$ composites [14,15,16]. The aim of this work has been the investigation of the synthesis of cellulose/$CaCO_3$ nanocomposites, their characterization and the assessment of their impact on the preparation of new polyethylene-cellulose/$CaCO_3$ composites. The preparation of cellulose/$CaCO_3$ nanocomposites involved the *in situ* synthesis of particles of $CaCO_3$ in the presence of cellulosic fibres. It has been reported that the carboxyl groups in cellulose pulp fibres are the main retention sites of several wet-end additives in pulp suspensions [17]. Besides, Dousi and co-workers [18] reported that carboxylated polymers stabilize the formation of calcite polymorphs. Thus we have undertaken a study using two distinct cellulosic substrates: hardwood bleached kraft pulp and carboxymethylated fibres.

Cellulose/$CaCO_3$ nanocomposite materials might be considered as potential reinforcing fillers in polymer matrix composites. Hitherto, practically no information is available on composites of thermoplastics like PE with cellulose/calcium carbonate materials.

This thesis is divided into four parts. In the first part it is presented a bibliographic review of the fundamental aspects of cellulose, calcium carbonate and composite materials. The second part describes the most relevant experimental methods used in this work. The third part presents the results and their discussion. Finally, the fourth part presents the major conclusions obtained in this research, as well as some lines to future work.

PART I – BIBLIOGRAPHIC REVIEW

1 CELLULOSE

Cellulose, the most abundant natural polymer on earth, is the main component of plant tissues and is known to be present in bacterial, fungal, algal species and even in animals [19]. This organic material has become a raw material of great economical importance since it is obtained from renewable resources and has specific properties such as non-toxicity, safe disposability after use, and good mechanical properties [2].

1.1 Cellulose Fibre Structure

Cellulose presents the most unique and simple structure in the field of polysaccharides. Its structure influences the course of chemical reactions and is responsible for the macroscopic properties of the polymer [2]. In order to describe and understand the structure of cellulose it is essential to distinguish three structural levels [2,20]:

(i) molecular level: chemical composition, steric conformation, molecular mass, presence of functional groups, intra- and intermolecular interactions;

(ii) supermolecular level: aggregation of chain molecules to elementary crystals and fibrils, degree of order;

(iii) morphological level: spatial position of the fibrillar aggregations in the fibres, existence of distinct cell wall layers, presence of voids or interfibrillar interstices.

1.1.1 Molecular Structure

Cellulose is a linear homopolymer composed of D-anhydroglucopyranose units linked together by β-(1→4)-glycosidic bonds. The repeating unit in cellulose consists in two consecutive anhydroglucose units, known as cellobiose unit, and every glucose unit is hence turned around the C(1)-C(4) axis by 180° with respect to its neighbours, giving to cellulose a 2-fold screw axis [1,20, 21]. The basic molecular structure of cellulose is illustrated in Figure 1. The pyranose rings are in the $^4C_1$-chair conformation (lowest energy conformation), with the $–CH_2OH$ and –OH groups, as well as the glycosidic bonds, in an equatorial position [22]. Each D-glucopyranose unit possesses free hydroxyl groups at C-2, C-3 and C-6 positions. The hydroxyl groups at both ends of the cellulose chain show different properties: the C-1 end has reducing properties, while the glucose end group with a free C-4 hydroxyl group is a non-reducing one [2].

The chain length of cellulose, i.e. the number of repeating anhydroglucose units (degree of polymerization, DP) differs widely depending on the origin and treatment of the raw material. For example, cellulose chains have a DP of about 10000 glucopyranose units in wood cellulose and 15000 in native cotton cellulose [21], while the DP of wood pulp fibres is in the range of 600-1500 [23].

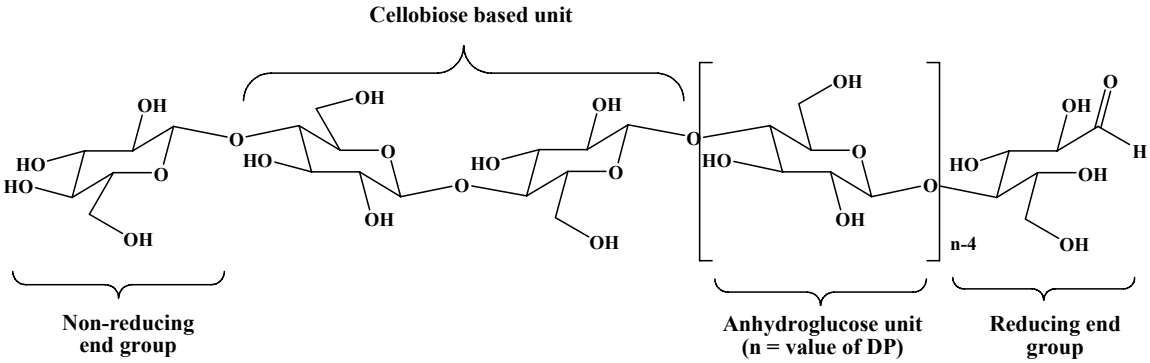

Figure 1: Cellulose molecular structure [2].

The molecular structure of cellulose is responsible for its characteristic properties: hydrophilicity, chirality, degradability, and broad chemical modifying capacity due to the high donor reactivity of the OH groups [1]. The three hydroxyl groups in each glucose unit of the cellulose molecule are able to undergo chemical reactions as well as to interact with other hydroxyl groups forming strong hydrogen bonds. In the solid state, cellulose molecules aggregate by means of intramolecular hydrogen bonds (OH-groups of adjacent glucose units in the same cellulose molecule link together) and intermolecular hydrogen bonds (OH-groups of adjacent cellulose

molecules link giving rise to supramolecular structures) [2,20]. The intramolecular hydrogen bonds (Figure 2) are formed between the hydroxyl groups on C(3) of one glucose unit and the pyranose ring oxygen O(5') of the neighboring glucose unit; and between the hydroxyl groups on the carbon atoms C(2) and C(6) [2,20]. The intermolecular hydrogen bonds (Figure 2) – predominant factor responsible for the interchain cohesion – are formed between the hydroxyls on the carbon atoms C(6) and C(3') [2,20].

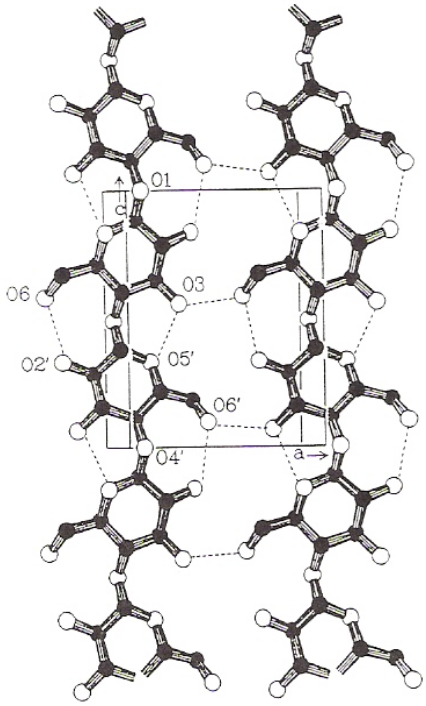

Figure 2: Most probable hydrogen bond patterns of cellulose I (002 plane) [20].

1.1.2 Supermolecular Structure

The supermolecular structure of cellulose is responsible for many of the cellulose chemical and physical properties. Various organization models of fibre structure have been proposed but, so far, the Fringe-Fibrillar model is the one that comes rather close to reality [2].

According to several authors, the basic element of the supermolecular structure of cellulose fibres is the so-called elementary crystallites [20], as illustrated in Figure 3. Strings of elementary crystallites are thus aggregated together in the form of elementary fibrils. Furthermore, bundles of elementary fribrils form microfibrils, in which highly ordered (crystalline) regions alternate with

less ordered (amorphous) regions – Figure 4. Microfibrils in turn build up into macrofibrils and these into cellulose fibres.

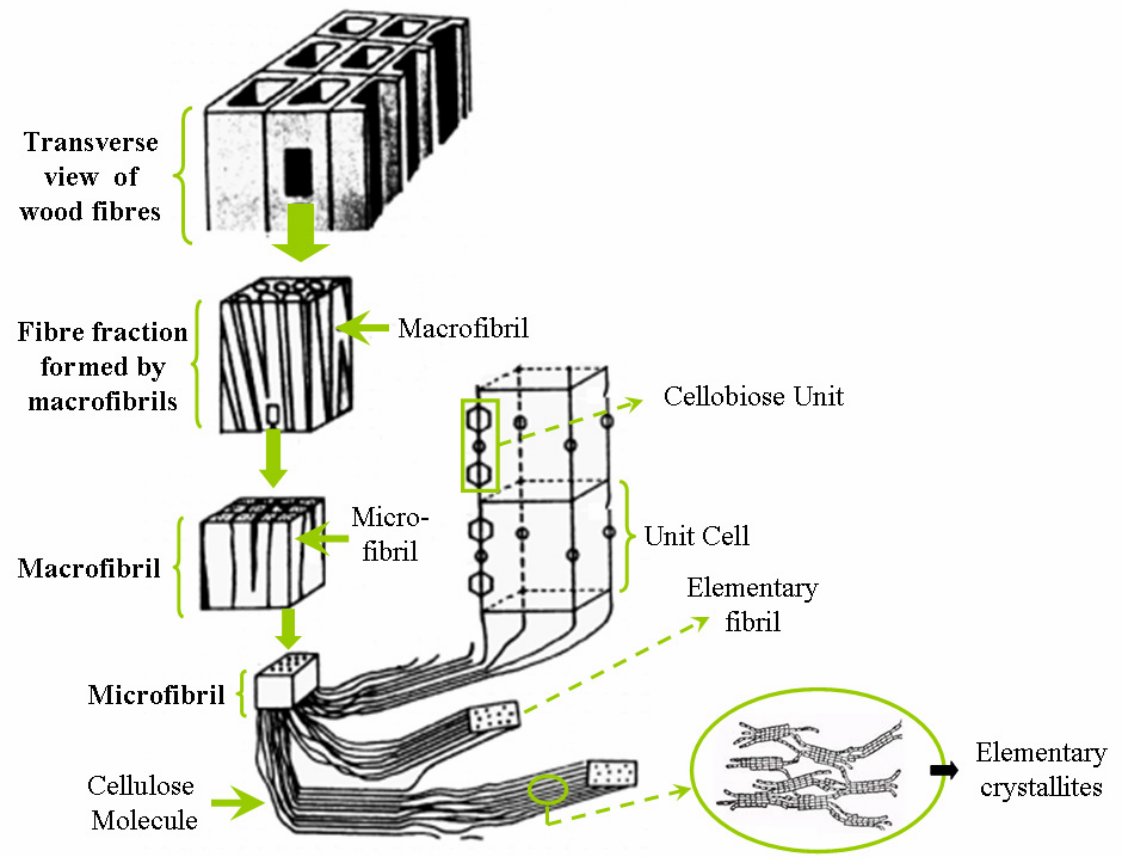

Figure 3: Microscopic structure of cellulose (Adapted from [20,23]).

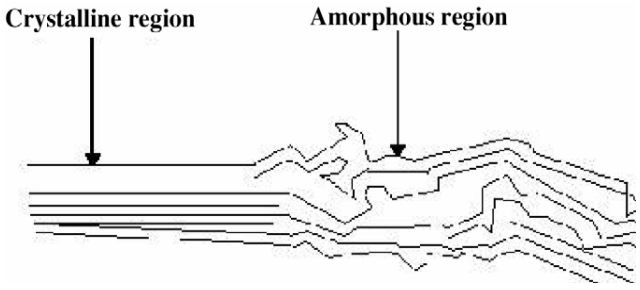

Figure 4: Cellulose elementary fibril morphology [24].

The elementary fibril is formed by the association of many cellulose molecules which are linked together in repeating lengths along their chains. Hence, in the crystalline state cellulose may be considered to be formed by identical repetition units, each one is termed as the unit cell (Figure 5). The unit cell of native cellulose or cellulose I is monoclinic, with dimensions of 0.835 nm for the a-axis, 1.03 nm for the b-axis, 0.79 nm for the c-axis and 84º for the β-angle [2]. The orientation of the cellulose molecules in the unit cell is still an issue under discussion. However, the Meyer and Misch model (Figure 5) proposes an anti-parallel orientation of the cellulose molecules in the unit cell, meaning that they are in a reverse position with respect to one another [20].

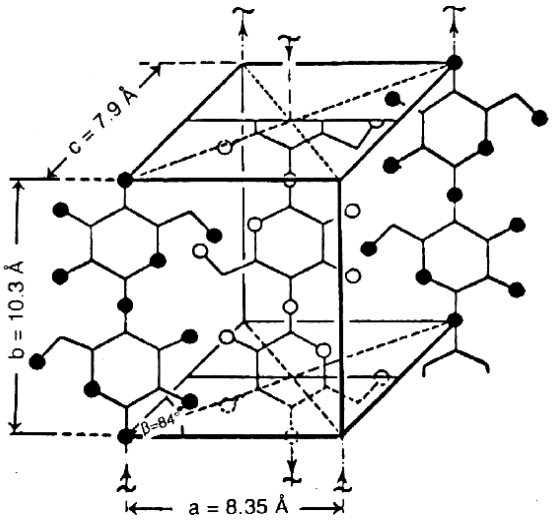

Figure 5: Unit cell of cellulose I according to the Meyer-Misch model [2].

Apart from the thermodynamically less stable cellulose I or native cellulose, this natural polymer can adopt other crystal structures which vary in unit cell dimensions and, probably, in chain polarity [1,2]. The polymorphism of cellulose crystal structure has been well documented in literature [2,19,20,22,25]. Hitherto, six polymorphs of cellulose are known (I, II, III_I, III_{II}, IV_I and IV_{II}) [22] and can be interconverted (Figure 6):

(i) **native cellulose or cellulose I**: there are two crystalline forms of cellulose I, designated as cellulose I_α and cellulose I_β and the crystalline component of cellulose I corresponds to a mixture of these two forms;

(ii) **cellulose II**: may be obtained from cellulose I by either regeneration (solubilisation of native cellulose in a solvent followed by reprecipitation by dilution in water) or mercerization (swelling of cellulose fibres in a concentrated aqueous alkali solution after removing the swelling agent);

(iii) **cellulose III**: celluloses III_I and III_{II} are formed from celluloses I and II, respectively, through treatment with liquid ammonia, and subsequent evaporation of ammonia;

(iv) **cellulose IV**: polymorphs IV_I and IV_{II} are prepared by heating celluloses III_I and III_{II} respectively [19,22,25].

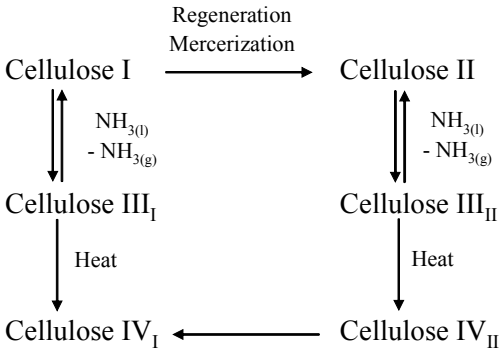

Figure 6: Polymorphic interconversion of cellulose [19,22].

The polymorphs of cellulose present different x-ray diffraction patterns as illustrated in Figure 7. Thus, the identification of the polymorphic form of cellulose is quite simple.

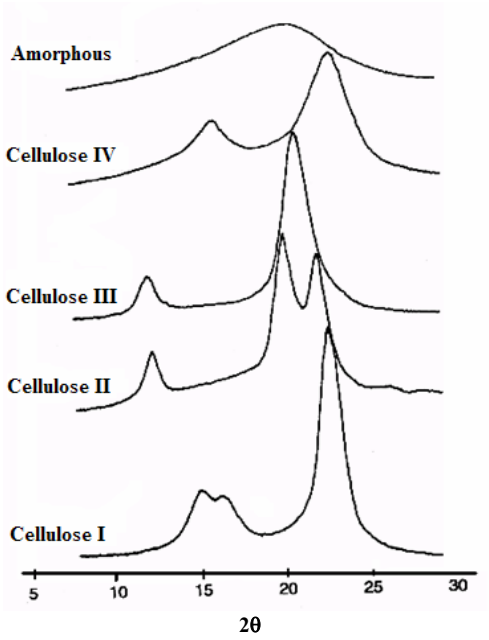

Figure 7: Typical X-ray diffraction patterns of amorphous cellulose, and celluloses I, II, III, and IV [26].

1.1.3 Fibre Cell Wall Structure

Cellulose is the vital component of all plant-fibres since it forms the skeleton of their cell walls. The morphology of the cellulose fibres is based on a hierarchy of fibrillar entities organized in layers differing in fibrillar texture [2]. The cell wall ultrastructure consists of four main layers: the middle lamella (ML), the primary wall (P), the secondary wall (S) and the warty layer (W), as illustrated in Figure 8. All these layers differ from each other in terms of structure and chemical composition.

The middle lamella (ML) with 0.2-1.0 μm of thickness is responsible for bounding the cells together and consists, in the mature state, mainly of lignin [20,21]. The outer layer of the cell – the primary wall (P) – with 0.1-0.2 μm of thickness is composed by cellulose, hemicelluloses, pectin, and protein and is entirely embedded in lignin [21]. The next inner cell wall layer is the secondary wall (S) that is formed by cellulose fibrils between which lignin and hemicelluloses are located [21]. Three distinct layers of the S wall can be recognized: S1 is the outer layer with 0.1-0.2 μm thick; S2 with 2-10 μm of thickness forms the main body of the fibre; and S3 is the inner layer with 0.1 μm thick [23]. Finally, the warty layer (W) located in the inner surface of the cell wall is a thin amorphous membrane with a still unidentified composition [21].

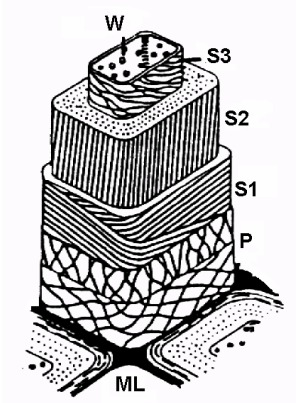

Figure 8: Diagram of cell wall organization [27].

1.2 Cellulose Modification

Cellulose exhibits a number of properties that make it a rather ideal fibrous polymer [2]. The most relevant properties are its hydrophilicity, biodegradability, broad chemical modifying capacity, and its formation of versatile semicrystalline fibre morphologies [1,2]. However, cellulosic fibres also display some limitations as a result of their polar and hydrophilic character.

The chemistry of cellulose is mainly the chemistry of the hydroxyl groups. The three reactive hydroxyl groups at the C-2, C-3, and C-6 atoms are, in general, accessible to the typical conversions of primary and secondary alcoholic OH groups [31]. The hydroxyl groups located in the crystalline regions with close packing and strong interchain bonding can be completely inaccessible under specific reaction conditions, while those in amorphous regions are highly accessible and react readily [21].

Cellulose is a fibrous substance insoluble in water and conventional organic solvents, but swellable in several polar protic and aprotic liquids [2]. This situation is an outcome of the crystalline nature of cellulose [28]. Both swelling and chemical modification are good tools to destroy the ordered structure of cellulose, i.e. to improve the accessibility of the molecules. Nevertheless, chemical modification provides a dominant route towards the production of innovative cellulose polymers with specific properties and their utilization in a wide range of applications. Cellulose derivatives constitute a very important part of the world market for polymers. Hitherto, there's a wide variety of routes for cellulose functionalization, as emphasized by the numerous reviews on the topic [29,30,31,32]. The functionalization of cellulose can either be done by homogeneous (dissolved cellulose) or heterogeneous reactions (cellulose in the solid or more or less swollen state), and both affect the supramolecular and morphological structure of cellulose [2]. Currently, most commercially available cellulose products are produced by heterogeneous reactions [1,2]. Additionally, the wide variety of cellulose derivatives are mainly produced by complete or partial esterification or etherification of the hydroxyl groups [2]. In both esterification and etherification reactions it is necessary a preswelling of the cellulose fibres in order to improve the accessibility of the hydroxyl groups for the later reaction. Two types of swelling of cellulose can be distinguished: intercrystalline, where the swelling agent penetrates only in the amorphous segments of cellulose, and intracrystalline, where the swelling agent penetrates the amorphous and affects the crystalline segments of cellulose [2,20]. Both swelling types result in the rupture of intermolecular bonds between the cellulose chains but, because of the limited solvation of the interaction compound formed, the intermolecular cohesion between cellulose chains are still preserved [2].

In this work, the use one of the most important cellulose ether – carboxymethylcellulose (CMC) – is of particular interest since it is known that carboxylated polymers stabilize the formation of calcite polymorphs, as reported by Dousi and co-workers [18]. Moreover, Isogai et al. [17] also showed that carboxyl groups in cellulose pulp fibres are the main retention sites of several wet-end additives in pulp suspensions.

The industrial production of carboxymethylcellulose involves a heterogeneous slurry of cellulose in a solvent that swells but does not dissolve neither the initial polymer nor the CMC obtained [33]. In general, this chemical modification occurs in two steps: the activation of cellulose by the aqueous sodium hydroxide solution, followed by the cellulose conversion to carboxymethylcellulose with monochloroacetic acid (MCAA) [34], as shown in Figure 9. The substitution of cellulose's hydroxyl groups with carboxymethyl groups results in significant improvement of accessibility; even water solubility is achieved when the degree of substitution ($0 \leq DS \leq 3$) is higher than 0.4, giving high viscosity in dilute solutions [34].

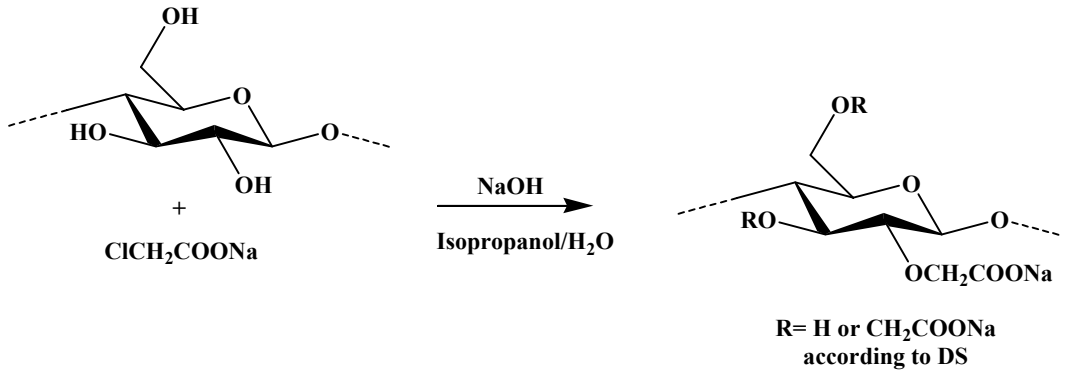

Figure 9: Reaction scheme of the carboxymethylation of cellulose in heterogeneous medium [34].

2 CALCIUM CARBONATE

Calcium carbonate is one of the most abundant minerals and has received much attention as a result of its industrial importance, diversity as a biomineral, and crystalline complexity. This mineral is a significant building material of natural hard tissues such as bones and teeth, and is extensively used as a filler in paints, plastics, rubber and paper.

2.1 Polymorphism and structural aspects

Calcium carbonate has three anhydrous crystalline polymorphic forms stable at ambient conditions: calcite, aragonite and vaterite. In addition to these crystalline forms, amorphous calcium carbonate (ACC) is also known. These polymorphs can adopt a variety of morphologies and have distinct solubility in water. The polymorphs of $CaCO_3$ are widespread minerals throughout nature, being vital inorganic components in the tissues and skeletons of many organisms, and a main constituent of sedimentary rocks.

Calcite (Figure 10) is the most thermodynamically stable polymorph of $CaCO_3$ at room temperature under normal atmospheric conditions and thus it is the most abundant form of calcium carbonate on earth surface. Natural calcite is relatively pure, being magnesium, ferrous and manganese ions common impurities. Besides, calcite has a rhombohedral crystal structure (Figure 10) with a space group *R3c* and $a = b = 4.990$ Å, $c = 17.061$ Å, $\alpha = \beta = 90^o$, and $\gamma = 120^o$ [35].

Aragonite (Figure 10) is a metastable phase of calcium carbonate that is effortlessly transformed into calcite by variations in environmental conditions. This polymorph of $CaCO_3$ has an orthorhombic crystal structure (Figure 10) with a space group *Pmcn* and $a = 4.9598$ Å, $b = 7.9641$ Å, $c = 5.7379$ Å, and $\alpha = \beta = \gamma = 90^o$ [36]. Aragonite is an interesting reinforcement material in composites due to its strength and needle-like morphology [37]. Besides, it is a vital biomaterial since it is hydrothermally transformed into biocompatible hydroxyapatite [38].

Vaterite (Figure 10) is the thermodynamically less stable crystalline form of calcium carbonate and is a scarce mineral in nature. The particles of this polymorph do not present well-defined morphologies, and frequently aggregate into spheroidal particles [39]. Vaterite has a hexagonal crystal structure (Figure 10) with a space group *P63* and $a = b = 4.13$ Å, $c = 8.48$ Å, $\alpha = \beta = 90^o$, and $\gamma = 120^o$ [35].

Finally, amorphous calcium carbonate (ACC) is a thermodynamically unstable form of $CaCO_3$. It is widely used by biological organisms as a temporary storage deposit for calcium and carbonate [40], but it is easily dissolved in water and with time transforms into a crystalline form.

Calcite mineral crystals [41]

Calcite crystal structure [42]

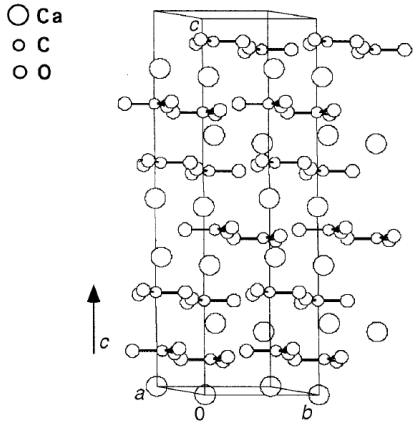

Aragonite mineral crystals [43]

Aragonite crystal structure [42]

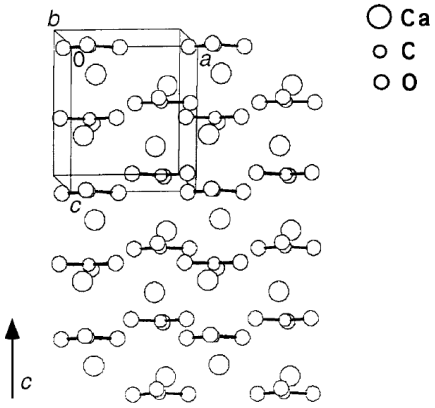

Vaterite mineral crystals [44]

Vaterite crystal structure [45]

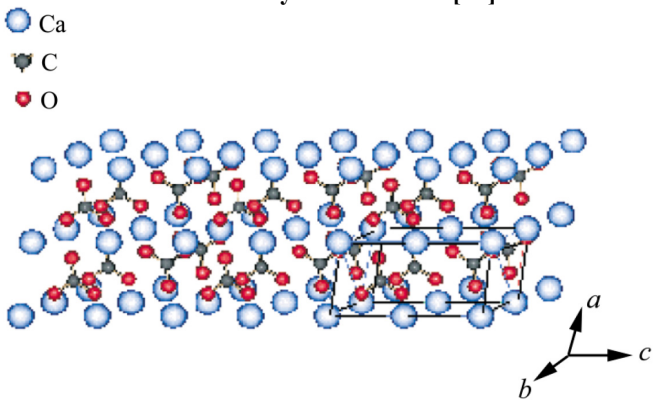

Figure 10: The biomineral crystals and crystal structure of calcium carbonate polymorphs.

2.2 Chemical routes to produce calcium carbonate

The use of calcium carbonate in numerous industrial applications is determined by the average particle size, the particle size distribution, the morphology, the specific surface area, the type of polymorph or the chemical purity [46]. Therefore, the ability to manufacture $CaCO_3$ with strictly defined characteristics is of enormous importance to industrial applications.

The knowledge of the key-controlling factors of crystallization (Figure 11) is crucial for the selective crystallization of the polymorphs [47]. The crystallization process of each polymorph comprises the competitive nucleation and crystal growth of the polymorphs, and the transformation from metastable to stable forms [47].

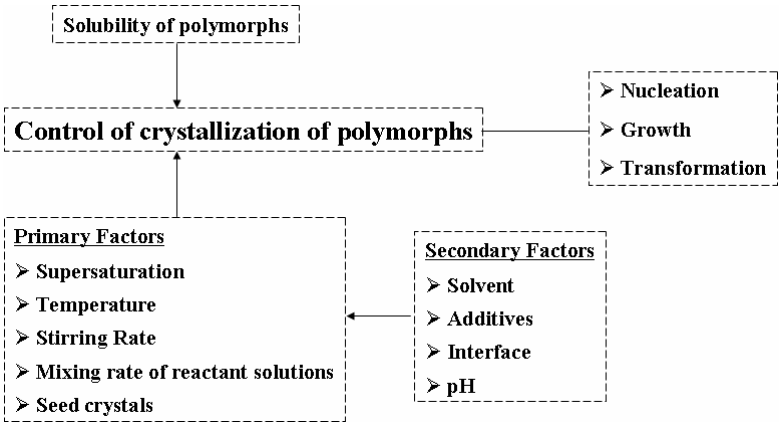

Figure 11: Scheme of controlling factors in crystallization of polymorphs [47].

The primary factors that influence the polymorphism of calcium carbonate are the concentration of the reactant solutions (supersaturation) [47,48], the reaction temperature [47], the stirring rate [49], the mixing rate of the reactant solutions [47], and the addition of polymorph seed crystals [50]. In turn, the secondary factors that influence the polymorphism of calcium carbonate are operational parameters such as solvents [51], additives [52,53,54], interfaces [55] and pH [49]. The solubility of each polymorph is also a factor that influences the crystallization process of $CaCO_3$ since it affects the supersaturation degree and allows the prediction of the relative thermodynamic stability and the direction of the transformation between the polymorphs [47].

The main routes to produce powders of $CaCO_3$ are shown in Figure 12. In industry, calcium carbonate is generally produced by bubbling carbon dioxide through an aqueous calcium hydroxide slurry – carbonation route [46,56]. However, most of the research has been done using the direct precipitation method with solutions of calcium and carbonate ions [47,57].

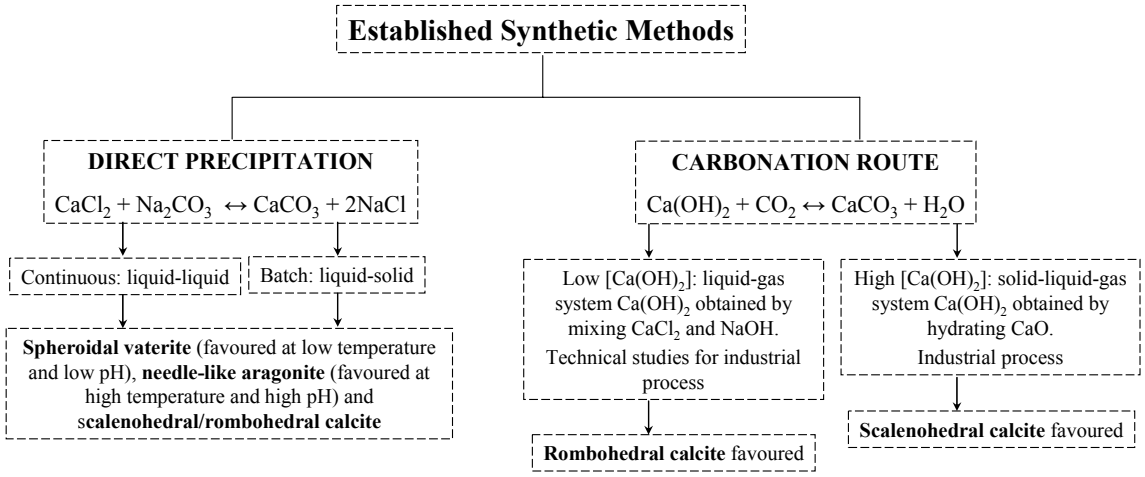

Figure 12: Most common established synthetic procedures for the controlled precipitation of $CaCO_3$ powders (Adapted from [46]).

2.2.1 Direct Precipitation

The direct precipitation is mainly used in laboratory due to its simplicity of operation and easy control of the experimental parameters. In this process, aqueous solutions containing calcium and carbonate ions are mixed, in alkaline medium, to form a calcium carbonate precipitate and ionic soluble species, as depicted by the following reaction:

$$CaCl_2 + Na_2CO_3 \rightarrow CaCO_3 + 2NaCl \qquad \textbf{(Reaction 1)}$$

The preparation of $CaCO_3$ using this method has been extensively reported. For example, Söhnel and Mullin [58] studied the precipitation process of $CaCO_3$ by mixing equimolar solutions of Na_2CO_3 and $CaCl_2$ at different concentrations in aqueous solution. They estimated the growth rate of calcium carbonate crystals by a desupersaturation method and discussed the effects of ionic impurities on the final crystal morphology. Morales et al. [59] investigated the precipitation of $CaCO_3$ at various $[Ca^{2+}]/[CO_3^{2-}]$ ratios by mixing Ca^{2+} and CO_3^{2-} solutions at 25°C. In another study, Morales and co-workers [60] explored the effect of solution pH on the $CaCO_3$ precipitation. Kawano et al. [48] investigated the formation process of calcium carbonate from highly supersaturated aqueous solutions of $CaCl_2$ and Na_2CO_3 at 20°C. Kitamura [47] discussed the effect of the supersaturation, the mixing rate of the reactant solutions and temperature, on the morphology and the crystallization of $CaCO_3$ polymorphs, between calcium chloride and sodium carbonate aqueous solutions.

The direct precipitation method of calcium carbonate is also used at an industrial level. An example is the $CaCO_3$ produced in the kraft pulp industry (Figure 13) as a by-product in the causticizing process used to manufacture sodium hydroxide.

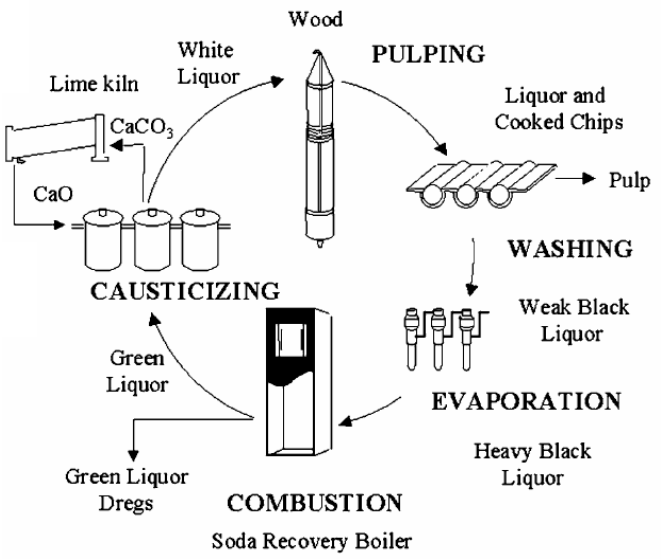

Figure 13: Causticizing process as a part of the pulp mill chemical recovery circuit [61].

The production of $CaCO_3$ in the chemical recovery process of sodium hydroxide in the kraft pulping process [49] is a special case of direct precipitation method in which calcium hydroxide reacts with sodium carbonate to produce a sodium hydroxide solution from which the calcium carbonate is precipitated:

$$Ca(OH)_2 + Na_2CO_3 \leftrightarrow CaCO_3 + 2NaOH \qquad \textbf{(Reaction 2)}$$

The available information regarding the crystallization of calcium carbonate in the causticizing process is scarce although there is a patent [62] on the process. One of the few reports on the crystallization of $CaCO_3$ in the causticizing reaction was done by Kitamura and co-workers [49], in which they investigated the controlling factor and the mechanism of the crystallization of calcium carbonate polymorphs by adding the Na_2CO_3 solution to the $Ca(OH)_2$ suspension. Konno and co-workers studied the mechanism for the crystallization process of aragonite [63]. These authors discussed the effect of NaOH on the aragonite precipitation in a batch and the continuous crystallization in the causticizing process in the paper industry [64].

2.2.2 Carbonation Route

The most interesting method in the industry to precipitate calcium carbonate is to bubble carbon dioxide gas through a slurry of calcium hydroxide. The formation of $CaCO_3$ from $Ca(OH)_2$ is usually represented by the following overall reaction:

$$Ca(OH)_2 + CO_2 \leftrightarrow CaCO_3 + H_2O \qquad \textbf{(Reaction 3)}$$

An important example of the carbonation route comes from the paper industry, where calcium carbonate (the so-called precipitated calcium carbonate (PCC)) is commonly used as filler in paper together with other additives to improve optical and physical properties.

The carbonation route is a useful industrial method in terms of environment preservation and effective use of mineral resources. Nevertheless, the control of the crystal shape and crystalline phase of $CaCO_3$ particles is particularly difficult [65].

The majority of the researches done using the carbonation method are technical studies related with the industrial process. For instance, Wang et al. [65] synthesized hydrophobic $CaCO_3$ nanoparticles by a carbonating route via an organic substrate inducing process (mixture of $Ca(OH)_2$ and $C_{18}H_{37}OPO_3H_2$ with CO_2/N_2 gas mixture). Xiang et al. [54] studied a modified carbonation process for the synthesis of super-fine $CaCO_3$ particles from a $Ca(OH)_2$ slurry, at room temperature, using a CO_2-air gas mixture. These researchers investigated the effect of the gas sparger and chemical additives on the particle size and morphology in the carbonation process. Gu et al. [66] reported a novel method to obtain calcium carbonate particles by direct contact of $Ca(OH)_2$ powders with supercritical CO_2. They converted dry $Ca(OH)_2$ powder to $CaCO_3$, with yields superior than 98%, due to the supercritical CO_2 containing water that passes over the dry $Ca(OH)_2$ powder. The investigation of Karagiozov and Momchilova [67] originated nano-sized particles of calcium carbonate by a chemical reaction in a microemulsion of water in oil. These researchers suggested that the CO_2 gas initiated a chemical reaction when inside the microemulsion droplet containing $Ca(OH)_2$, thus originating a slightly soluble product ($CaCO_3$).

Generally, $CaCO_3$ powders synthesized by the carbonation route are a mixture of various crystalline polymorphs with extremely agglomerated particles and anisotropic distribution of sizes. In order to overcome these drawbacks, new methods based on the generation of carbon dioxide from organic precursors have been developed. An example is the synthesis process of amorphous calcium carbonate (ACC) via hydrolysis of alkyl carbonates such as dimethyl carbonate (DMC). This organic precursor is a green reagent with low toxicity and high biodegradability, which is

easily transformed into methanol and carbon dioxide by base- or acid-catalyzed hydrolysis [68]. One of the few studies on the CO_2-prodution by base-catalyzed hydrolysis of dimethyl- and diethyl-carbonate was done by Faatz and co-workers [69,70]. These researchers obtained spherical particles of ACC with monodispersed distribution of diameters under quiescent conditions. Besides, they observed that the by-products of the decomposition of these dialkyl-carbonates (methanol or ethanol) do not interfere with nucleation and growth of calcium carbonate, at least within the concentration range in which they appear. In another study, Faatz et al. [71] evaluated the physical properties of amorphous $CaCO_3$ colloidal spheres of monomodal size distribution. Guillemet and co-workers [72] used the slow release of CO_2 by alkaline hydrolysis of DMC in water to prepare particles of ACC from $CaCl_2$. These ACC particles were stabilized against coalescence in the presence of very small amounts of double hydrophilic block copolymers composed of poly(ethylene oxide) and poly(acrylic acid) blocks. More recently, Gorna et al. [73] investigated the precipitation of ACC from strong alkaline solution of $CaCl_2$ at room temperature using the hydrolysis of dimethyl carbonate as the internal source of CO_2. These researchers optimized the DMC method in order to obtain multigram amounts of calcium carbonate per batch.

3 COMPOSITE MATERIALS

In general, composites are composed of two or more constituent materials with considerably different chemical or physical properties [74]. Composites are materials with inhomogeneities on length scales larger than the atomic scale but are essentially homogeneous at macroscopic length scales or at least at some intermediate length scales [75].

Composite materials exist in both Nature and among engineered materials [75]. As far as man-made materials are concerned, the use of composite materials started since ages. According to the biblical Book of Exodus, Moses's mother used a kind of fibre-reinforced composite made from rushes, pitch and slime to build the ark [76]. Another example comes from the opium war (more than 1000 years ago) where the Chinese people used a kind of mineral particle-reinforced composite made from gluten rice, sugar, calcium carbonate and sand to build castles to defend themselves against invaders [76].

3.1 Overview

Composites comprise a very broad and important class of engineering materials with a world annual production of over 10 million tonnes [77]. These materials have attracted the interest of a number of researchers since they offer unpaired mechanical, optical, electrical and thermal properties which allow them to be applied in several areas such as mechanics, optics, electronics, ionics, energy, environment, biology and medicine [74,77]. Numerous composite materials with great potential for high added-value applications have been developed over the past few decades. The paramount reason of this development is the enormous versatility of the synthetic processes and the almost endless choices of feasible combinations that can be employed to obtain composite structures, as emphasized by the numerous reviews on the topic [3-6,76,78-80]. For example, Mohanty, Misra and Hinrichsen [4] published an interesting review article on the current development of biocomposites with a broad outline of discussion on structural parts of some important biofibres (jute, ramie, kenaf, etc) and the current development of different biodegradable polymers (cellulose acetate, poly(lactic acid), starch, etc). An interesting review article on recent advances in nanocomposites research was published by Thostenson, Li and Chou [78]. These researchers emphasized the knowledge in processing, characterization, and analysis/modelling of

nanocomposites as well as promising techniques for processing precursors for macroscopic nanocomposites. In another review article, Tjong [79] provided a comprehensive review on the effects of nanoclays, nanoceramic particles and carbon nanotubes on the structure and mechanical properties of semicrystalline and glassy thermoplastics, elastomers and epoxy resins. An interesting report on polymer blends and composites from renewable resources have been presented by Yu, Dean and Li [76]. Recently, Ray and Easteal [80] provided a brief overview on the advances in polymer-clay nanocomposites (PCN) with focus on nanocomposite structures, synthesis, properties, applications, and future markets.

3.2 Cellulose-based Composites

Cellulose and its derivatives are promising raw materials for the synthesis of composites, namely because of their environmentally friendly nature. Therefore, the study of these composite materials became an expanding field of investigation, as highlighted by the significant amount of research articles on the topic [3-12]. Researchers have developed composites in which cellulose and cellulose derivatives were used either as filler [3-6] or matrix [7-12].

An important review article concerning natural (cotton, jute, sisal, etc) and man-made (rayon) cellulose fibre reinforced plastics has been presented by Bledzki and Gassan [5]. In another paper, Eichhorn and co-workers [6] summarized a number of international research projects being undertaken to further understand the mechanical properties of natural cellulose fibres and composite materials. Recently, a review article about biofibres and biocomposites has been published by John and Thomas [3]. These researchers reviewed several aspects of cellulosic fibres and biocomposites, new developments dealing with cellulose based nanocomposites, as well as some examples of the applications of cellulosic fibre reinforced polymeric composites.

Barata et al. [12] studied the growth of $BiVO_4$ particles in cellulosic fibres by in situ reaction. According to their research the $BiVO_4$ particles grow from nucleation sites located in cell wall structure and inside the lumen of fibres. Marques and co-workers [9] prepared TiO_2/cellulose nanocomposites through the titanyl sulphate hydrolysis in acidic medium in the presence of cellulose fibres. They reported that cellulose fibres promote the nucleation and growth of TiO_2 particles. In another study, Pinto and co-workers [8] reported novel SiO_2/cellulose nanocomposites obtained by *in situ* synthesis and *via* polyelectrolytes assembly. The former method yielded homogeneously coated SiO_2/cellulose nanocomposites, while the latter method originated nanocomposites containing discrete and morphological well-defined SiO_2 nanoparticles at the

cellulosic fibres surfaces. Besides wood cellulose fibres, bacterial cellulose (BC) hydro-gel has also been used as matrix. For instance, Maeda et al. [81] developed BC/silica composites by the sol-gel method. The BC hydro-gel was immersed in an aqueous solution of silanol derived from tetraethoxysilane, which is converted to silica in situ in the BC hydro-gel matrix. These researchers found that deposited silica between BC micro-fibrils reinforced the composites. In an interesting research Pinto et al. [10] investigated two synthetic routes for nanocomposites containing gold nanoparticles attached onto wood or bacterial cellulosic fibres. Their research showed that wood or bacterial cellulose fibres are both good templates for nucleation and growth of inorganic particles of gold. Besides, the good optical features of these Au/cellulosic fibres nanocomposites make them suitable for security paper applications.

Additionally to the use of cellulose either as matrix or filler in composite materials, both filler and matrix can be made of cellulose or its derivatives [82-85]. For instance, Matsumura and Glasser [82,83] prepared a cellulosic composite by hot compaction in which the thermoplastic cellulose hexanoate phase formed a matrix reinforced with the core cellulose I. Nishino, Matsuda and Hirao [84] were the first to report the development of an all-cellulose composite in which the incorporated fibres and the matrix were both made from cellulose. Their composite was prepared by impregnating a cellulose solution into uniaxially aligned cellulose fibres. Despite the excellent mechanical and thermal properties of this all-cellulose composite, it was difficult to impregnate the cellulose solution into fibres. In a later study, Nishino and Arimoto [85] prepared all-cellulose composite from conventional filter paper by converting a selective dissolved fibre surface into a matrix. The tensile strength of these composites was comparable or even higher than those of conventional glass-fibre-mat-reinforced composites.

3.3 Cellulose/$CaCO_3$ Composites

Recently, several authors [8-12] have reported that cellulosic fibres can be efficient hydrophilic substrates in the nucleation and growth of inorganic particles in aqueous medium. Bearing this in mind together with the fact that paper can be considered to be a composite obtained by blending cellulose fibres, mineral additive particles ($CaCO_3$, kaolin and TiO_2) and other organic additives, cellulose/calcium carbonate composites can be regarded as potentially interesting materials with attractive properties. However, the information concerning composite materials obtained by the chemical or physico-chemical assembly of cellulose and calcium carbonate is very limited. One of the first studies dealing with cellulose/$CaCO_3$ composites was carried out by Fimbel and Siffert

[14] in which they investigated the interaction of calcite with cellulose fibres in aqueous medium. These researchers observed that the surface charge of cellulose is the key parameter of adsorption, and that $CaCO_3$ particles are efficiently adsorbed. Besides, cellulose surface is saturated at concentrations of 3 g of $CaCO_3$ per 100 cm^3 of suspension, and the quantity of $CaCO_3$ retained by the fibres is 1.4 g/g of dry cellulose. In another interesting investigation, Dalas et al. [15] showed that the use of cellulose powder as a substrate favours the overgrowth of calcite crystals from stable supersaturated solutions at pH 8.50 and at 25^{o}C. In addition, the selective deposition of calcite on cellulose is probably done by the formation of active sites at ionisable functional groups (-OH). Another example is the research work done by Subramanian and co-workers [16] that produced composites of PCC (precipitated calcium carbonate) and pulp by co-precipitating PCC in pulp suspension. The main conclusion of their study is that the co-precipitation technique increases the internal bond strength of fine paper, when compared to the conventional blending of cellulose fibres and $CaCO_3$ particles.

The knowledge that carboxyl groups in cellulose pulp fibres are the main retention sites of several wet-end additives in pulp suspensions [17] together with the fact that carboxylated polymers stabilize the formation of calcite polymorphs [18], led us also to the investigation of carboxymethylcellulose/$CaCO_3$ composites. So far, the available information on the topic of CMC/$CaCO_3$ composites is very scarce. As an example, Backfolk et al. [86] investigated the aspects on the interaction between sodium carboxymethylcellulose (NaCMC) and $CaCO_3$ and the relationship to specific site adsorption. According to this study, the mechanisms of interaction of NaCMC in $CaCO_3$ suspensions are mainly an association between NaCMC and Lewis acid sites on the $CaCO_3$ surface and the formation of NaCMC-Ca^{2+} complexes in the bulk solution. Furthermore, the adsorption of NaCMC onto $CaCO_3$ is essentially entropy-driven by an endothermic reaction.

Theoretically, every innovative material needs at least one potential application to be considered a meaningful material. Thus, cellulose/$CaCO_3$ nanocomposites might be considered a potential reinforcing element in polymer matrix composites. Composite materials with polymeric matrices have attracted attention in recent years due to their interesting properties. Therefore, much work has focused on developing composites using various polymers like, for instance, polyethylene (PE) [87-101].

Polyethylene (PE) is a linear non-biodegradable thermoplastic polymer that exhibits good chemical stability, biocompatibility, and wear resistance. It is extensively used in prosthesis components for hip and knee total joint replacement. It is a well known material because it is one of the most widely used plastic for bottles and containers due to its low cost, high water barrier and ease of processing.

The low-cost versatility of polyethylene makes it an extensively used polymer. Therefore, a large production of waste PE materials are being produced which, in turn, are causing serious environmental problems since PE takes a long time to decompose. In order to reduce this problem and also the production costs, polyethylene is often filled with a variety of materials that make it suitable for various applications. For instance, starch [87,88], wood-fibre [89,90], graphite [91], PVdF-HFP (poly(vinylidene fluoride hexafluopropylene)) [92], sawdust [93], silicate [94], and hydroxyapatite [95] have been used to produce PE-based composites. In addition, calcium carbonate [73,96,97] and cellulose [98-100] are also common fillers for PE-based composites. To our knowledge practically no information is available on composite materials of polyethylene reinforced with cellulose/$CaCO_3$ nanocomposites.

One of the main concerns of blending nonpolar polymers, like PE, with polar materials, such as natural fibres, is the formation of aggregates during processing which originates weak fibre/matrix interactions. In order to improve interfacial adhesion, compatibilizers have frequently been used. Polyethylene-*graft*-maleic anhydride (Figure 14), PE-g-MA, is a very important compatibilizing agent in the enhancement of compatibility between nonpolar PE and polar materials.

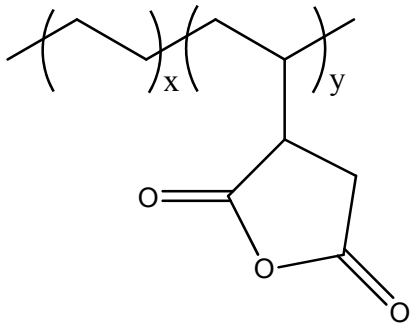

Figure 14: Polyethylene-*graft*-maleic anhydride.

Several studies have been done aiming to evaluate the compatibilizing effect of PE-g-MA on cellulose [99,100] and $CaCO_3$ [101]. Palaniyandi and Simonsen [99] investigated the physico-mechanical properties of cellulose-filled HDPE (high density polyethylene) in the presence of compatibilizers, PE-g-MA and AKD/PMDI (alkyl ketene dimmer/polymethylene diphenyl diisocyanate). They observed that the presence of both compatibilizers facilitated PE crystallization resulting in an increase in the matrix crystallinity. Fendler and co-workers [100] have discussed the interrelation between composition, morphology, thermal history, mechanical and barrier properties to oxygen and limonene of composites of HDPE/PE-g-MA/cellulose fibres of significant interest in, among others, food packaging applications. Wang and co-workers [101] reported that PE-g-MA

shows good compatibilizing effects on the high density PE and calcium carbonate system (HDPE/$CaCO_3$) which improved the mechanical properties of the composite materials.

PART II – EXPERIMENTAL

1 REAGENTS AND GENERAL PROCEDURES

1.1 Reagents

Acetic acid glacial (CH_3COOH) was purchased from Panreac (Product No.131008).

Acetone (CH_3COCH_3) pro analysis was supplied by Fisher Scientific (Product No. A/0600/17).

Calcium chloride anhydrous ($CaCl_2$, 93%) was acquired from Sigma (Product No. C-1016).

Dimethylcarbonate [$(CH_3O)_2CO$, 99%] was purchased from Aldrich (Product No. D15,292-7).

Ethanol Absolute (C_2H_6O) was supplied by Riedel-de Häen (Product No. 32221).

Isopropanol (C_3H_8O, ≥ 99%) was acquired from Fluka (Product No.59310).

Low density polyethylene, LDPE, [$H(CH_2CH_2)_nH$] in the form of pellets with a melting index of 25 g/10 min (190ºC/2.16 kg), a melting point of 116ºC and a density of 0.925 g/mL at 25ºC was purchased from Aldrich (Product No. 428043).

Monochloroacetic acid ($C_2H_3ClO_2$, ≥ 99%) was supplied by Fluka (Product No.24510).

Polyethylene-*graft*-maleic anhydride (PE-g-MA) in the powder form with ~3wt.% maleic anhydride and 1700-4500 cP (140ºC)(lit.) of viscosity was purchased from Aldrich (Product No. 456632).

Sodium hydroxide (NaOH, 97%) in the form of pellets was acquired from Acros Organics (Product No.424335000).

1.2 Cellulose Fibres

The wood cellulose fibres used in this study were *Eucalyptus globulus* ECF bleached kraft pulp supplied by a Portuguese pulp mill. All the fibres were disintegrated and washed with distilled water before use.

1.3 Carboxymethylcellulose Fibres

Carboxymethylcellulose (CMC) fibres were prepared by the etherification reaction of cellulose with monochloroacetic acid. Air-dried cellulose fibres (3g) were suspended in isopropanol (80 ml) and then a sodium hydroxide aqueous solution (8 ml, 30% w/w) was added dropwise during 30 minute at room temperature. The mixture was then stirred during 1 hour. After this, monochloroacetic acid (4g or 1g) was added in small portions during 30 minutes. The mixture was placed on a water bath at 25º or 45ºC for 10 min or at 55ºC for 3 hours with constant stirring. Then it was filtered, suspended in ethanol (200 ml, 80% v/v) and neutralized with acetic acid (ca. 30 ml). The final product was washed three times with ethanol (500 ml, 80% v/v), twice with absolute ethanol, and dried at room temperature.

The carboxymethylcelulose samples are listed in Table 1.

Table 1: Experimental plan describing CMC samples

Sample	Description
CMC I	3g cellulose / 1g MCAA / 10 min at 25ºC
CMC II	3g cellulose / 1g MCAA / 10 min at 45ºC
CMC III	3g cellulose / 4g MCAA / 3 hours at 55ºC

2 SYNTHESIS OF CELLULOSE/$CaCO_3$ NANOCOMPOSITES

The synthesis of $CaCO_3$ particles was performed based on the method reported by Faatz et al. [69], in which the precipitation of $CaCO_3$ takes place as a result of the release of carbon dioxide by the hydrolysis of dimethylcarbonate. In this work this synthesis was adapted to the formation of $CaCO_3$ in the presence of cellulosic fibres.

The preparation of the unmodified and modified cellulose/$CaCO_3$ nanocomposites started with the addition of 80 mg of cellulose fibres to a solution of 80 ml of distilled water, 111 mg of calcium chloride and 420 μl of dimethylcarbonate. This mixture was vigorously stirred during 12 hours at room temperature. The precipitation started after adding 20 ml of sodium hydroxide solution (0.5 M) to the reaction medium. A few minutes later the nanocomposite was removed from the reaction mixture by filtration, washed with acetone and dried at 40°C.

The effect of several reaction parameters on the characteristics of the nanocomposites was investigated. These parameters include reaction time (2.5, 3.5, 5.0 and 7.5 min) and temperature (25 and 70°C), fibre quantity (0.1 and 1%), and extent of cellulose modification. The experimental conditions used to prepare the nanocomposites are listed in Table 2. In order to produce enough nanocomposite for the preparation of PE-based composites and for further characterization, the synthesis process was scaled-up to 10g of cellulose (nanocomposites N and O).

Table 2: Experimental conditions used for the preparation of cellulose/$CaCO_3$ nanocomposites

Nano-Composite	Substrate	Time (min)	Temperature (^oC)	Consistency (%)[a]	Carboxyl Content (mmol/g)
A	Cellulose	2.5	25	0.1	0.10
B	Cellulose	3.5	25	0.1	0.10
C	Cellulose	5.0	25	0.1	0.10
D	Cellulose	7.5	25	0.1	0.10
E	Cellulose	3.5	70	0.1	0.10
F	Cellulose	3.5	25	1.0	0.10
G	Cellulose	5.0	25	1.0	0.10
H	CMC I	3.5	25	0.1	0.49
I	CMC I	5.0	25	0.1	0.49
J	CMC II	2.5	25	0.1	0.83
K	CMC II	3.5	25	0.1	0.83
L	CMC II	5.0	25	0.1	0.83
M	CMC II	7.5	25	0.1	0.83
N[b]	Cellulose	3.5	25	1.0	0.10
O[b]	CMC I	3.5	25	1.0	0.49

[a] The consistency of the reacting suspension is the ratio between the mass of fibres and the mass of suspension; [b] Nanocomposites prepared under scale-up conditions.

3 PREPARATION OF POLYETHYLENE-CELLULOSE/$CaCO_3$ COMPOSITES

Polyethylene-cellulose/$CaCO_3$ composites were made by melt-blending, using a mixer Brabender W30 EHT – Plastograph EC (Figure 15) at 170ºC with a screw speed of 100 rpm during 10 min. Different mixtures with a filler content of 15 and 30%, and a compatibilizer content of 0 and 2% were prepared (Table 5).

Test specimens were prepared on Haake MiniJet II Injector – Thermo Scientific (Figure 16) with cylinder and mould temperatures of 170 and 90°C, respectively. The injection pressure was 400 bar applied during 10 seconds and the post-pressure was 200 bar applied during 4 seconds.

Figure 15: Mixer Brabender W30 EHT – Plastograph EC.

Figure 16: Haake MiniJet II Injector – Thermo Scientific.

4 CHARACTERIZATION METHODS

The cellulose and carboxymethylcellulose fibres were analysed for carboxyl content and characterized by infrared spectroscopy (IR), x-ray diffraction (XRD), thermogravimetry (TGA) and scanning electron microscopy (SEM). In turn, the nanocomposites of cellulosic fibres and calcium carbonate were characterized by inductively coupled plasma-atomic emission spectrometry (ICP-AES), infrared spectroscopy (IR), x-ray diffraction (XRD), scanning electron microscopy (SEM), thermogravimetry (TGA), time-of-flight secondary ion mass spectrometry (ToF-SIMS) and x-ray photoelectron spectroscopy (XPS). Finally, the characterization of PE-based composites was performed by scanning electron microscopy (SEM), differential scanning calorimetry (DSC) and dynamic mechanical analysis (DMA).

4.1 Carboxyl Content

The content of carboxyl groups of the unmodified and modified celluloses were determined by the TAPPI Test Method T 237 om-93 [102]. The fibres were extracted with a dilute solution of hydrochloric acid (0.1M), washed with distilled water, reacted with sodium bicarbonate-sodium chloride solution (0.01M $NaHCO_3$ and 0.1M NaCl), and filtered. The filtrate was then titrated with a dilute solution of hydrochloric acid (0.01M) to methyl red end point.

4.2 Infrared Spectroscopy

The FTIR-ATR spectra were taken with a Brucker IFS 55 FTIR Spectrometer equipped with a single horizontal Golden Gate ATR cell. Their resolution was $8cm^{-1}$ after 128 scans.

4.3 Inductively Coupled Plasma-Atomic Emission Spectrometry

The concentration of calcium in the nanocomposites was analyzed by Inductively Coupled Plasma-Atomic Emission Spectrometry (ICP-AES) on a Jobin Yvon, JY 70 plus.

4.4 X-Ray Diffraction

The X-Ray diffraction (XRD) measurements were performed on a Philips X'Pert MPD diffractometer using Cu Kα radiation. All samples were gently pressed into pellets using a laboratory press in order to be analyzed.

4.5 Scanning Electron Microscopy

Scanning Electron Microscopy (SEM) micrographs were obtained using a low voltage microscope (HITACHI SU-70) operated at 2.0 and 4.0 kV, or using a high voltage microscope (HITACHI S4100) operated at 25.0 kV. Samples were previously coated with carbon using an EMITECH K950 coating system.

4.6 Thermogravimetric Analysis

Thermal decomposition temperatures were determined by thermogravimetric analyses (TGA) on a Shimadzu TGA-50 analyser equipped with a platinum cell. The thermograms were run under nitrogen atmosphere at constant heating rate of 10°C/min from the temperature of 20-800°C.

4.7 Differential Scanning Calorimetry

The differential scanning calorimetry (DSC) analysis was carried out on a Shimadzu DSC-50. Samples of 5-6 mg were heated from 25ºC to 200°C at 10°C/min in aluminium DSC capsules. The enthalpy of melting (related with the weight of PE in the sample) was used to determine sample crystallinity using the following relation:

$$X_C = \frac{\Delta H_m}{\Delta H_0} \times 100 \qquad \textbf{(Equation 1)}$$

where X_c is the crystalline fraction, ΔH_m is the enthalpy of melting measured by DSC and ΔH_0 is the enthalpy of melting for 100% crystalline polyethylene (taken as $\Delta H_0 = 293$ J/g [103,104]).

4.8 Dynamic Mechanical Analysis

Dynamic mechanical analysis (DMA) experiments were carried out in a Tritec 2000 Dynamic Mechanical Analyzer – Triton Technology, at a constant frequency of 1 Hz from -70°C to 120°C at a heating rate of 4°C/min. The test specimens were prepared on Thermo Haake MiniJet II and cut into rectangles of 2 mm length, 4 mm width and 1 thickness, so that they could be analysed.

4.9 Time-of-Flight Secondary Ion Mass Spectrometry

Secondary ion spectra and images were recorded using a Physical Electronics ToF-SIMS TRIFT II spectrometer (Laboratory of Fibre and Cellulose Technology, Åbo Akademi University, Turku, Finland) using a primary ion beam of $^{69}Ga^+$ liquid metal ion source (LIMS) with 15kV applied voltage, 600 pA aperture current and a bunched pulsed width of 20 ns was used in positive mode. A raster size of 200 μm x 200 μm and at least three different spots were analyzed on each sample. Surface distribution of calcium ions was obtained with the best spatial resolution using the ion gun operating at 25 kV, 600 pA of aperture current and an unbunched pulse width of 20 ns. Spectra and images were acquired for 8 minutes with a fluency of ~10^{12} ions/cm^2, ensuring static

conditions. Charge compensation was performed using an electron flood gun pulsed out of phase with the ion gun.

4.10 X-Ray Photoelectron Spectroscopy

X-Ray photoelectron spectra were obtained with a Physical Electronics PHI Quantum 2000 ESCA instrument (Laboratory of Fibre and Cellulose Technology, Åbo Akademi University, Turku, Finland) equipped with a monochromatic Al*K* α X-ray source and operated at 25 W, with a combination of electron flood gun and ion bombarding for charge compensation. The photoelectron collection was at 45º in relation to the sample surface and the spot size was 500 μm × 400 μm. At least three different spots were analyzed on each sample. The pass energy was 187.85 and 23.50 eV for low and high resolution, respectively. Curve fitting of C1s peak was performed using a Shirley background and the following binding energies, relative to C1 position (C – C, C – H), were employed for the respective groups: 1.7 ± 0.2 eV for C2 (C – O), 3.1 ± 0.3 eV for C3 (O – C – O or C = O), 4.6 ± 0.3 eV for C4 (O = C – O), 5.6 ± 0.3 eV for C5 (CO_3^{2-}), 8.6 ± 0.3 eV for C6 and 10.6 ± 0.3 eV for C7.

PART III – RESULTS AND DISCUSSION

1 CHARACTERIZATION OF THE CELLULOSIC SUBSTRATES

The cellulose substrates used in this study were mainly of two kinds: hardwood bleached kraft pulp and carboxymethylated fibres. They were analysed for carboxyl content and characterized by IR, XRD, TGA and SEM.

1.1 Carboxyl Content

Generally, the cellulosic fibres have quite low carboxyl groups (introduced mainly during cellulose processing, namely bleaching processing) which mean that they have low chelating capability. In order to overcome this drawback, cellulose fibres are usually submitted to chemical modification. The functionalization of cellulose by introducing carboxyl groups is very important since they are potential nucleation centres that increase cellulose accessibility and surface reactivity. The carboxymethylation of cellulose in heterogeneous medium is an effective way to introduce carboxyl groups on the surface of cellulose fibres.

Figure 17 shows the carboxyl contents of cellulose and the different CMC fibres prepared. The obtained carboxyl content for cellulose (0.10 mmol/g) is in the typical range for bleached kraft pulp [105,106], while the carboxyl content of the three CMC samples reached a maximum value of 1.83 mmol/g when 4g of MCAA was used and the reaction was performed at 55ºC for 3 hours. Any other reaction conditions (Table 1) gave products of lower carboxyl contents. It is worth to mention that higher contents of carboxyl groups originated CMC fibres with higher affinity towards water.

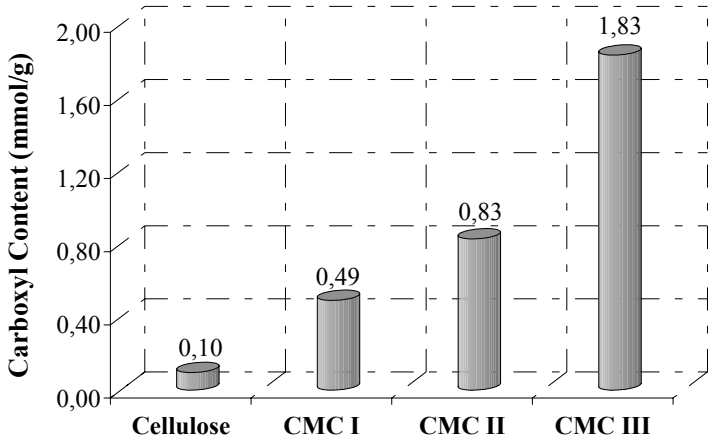

Figure 17: Carboxyl content of cellulose and carboxymethylcellulose fibres (See Table 1 for CMC identification).

1.2 Infrared spectroscopy

Infrared spectroscopy has been used for a long time as a tool to characterize cellulose. A typical example of IR spectrum of cellulose with the main absorption bands of this natural polymer is illustrated in Figure 18. The most important absorption bands occur at 3200 –3400 cm^{-1} (OH stretching), 2900 cm^{-1} (CH stretching), 1426– 1430 cm^{-1} (CH_2 bending), 1350– 1355 cm^{-1} (CH bending), 1310 cm^{-1} (OH bending), 1025 cm^{-1} (CO stretching) and 900–910 cm^{-1} (CH bending) [2].

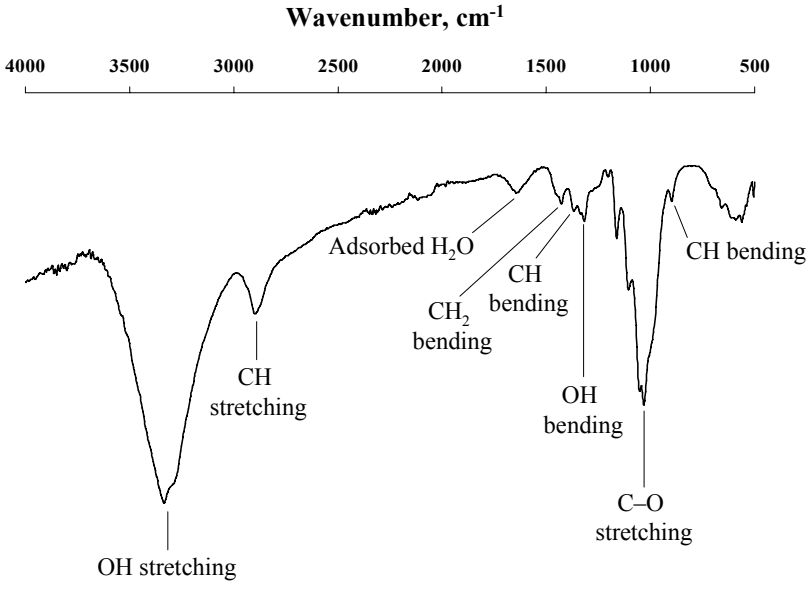

Figure 18: FTIR-ATR spectrum of cellulose.

The IR spectra of the CMC samples showed the typical absorption bands of the cellulose backbone, as well as the characteristic absorption bands of carboxyl groups [2]: anti-symmetrical vibration of ionized carboxyl groups, ν_{as}(COO-) at 1590–1640 cm^{-1} and vibration of carboxyl groups, ν(COOH) at 1705–1735 cm^{-1}. The emergence of these bands provided an unambiguous evidence of the occurrence of the carboxymethylation of cellulose. The infrared spectra of CMC I, CMC II and CMC III are shown in Figure 19 .

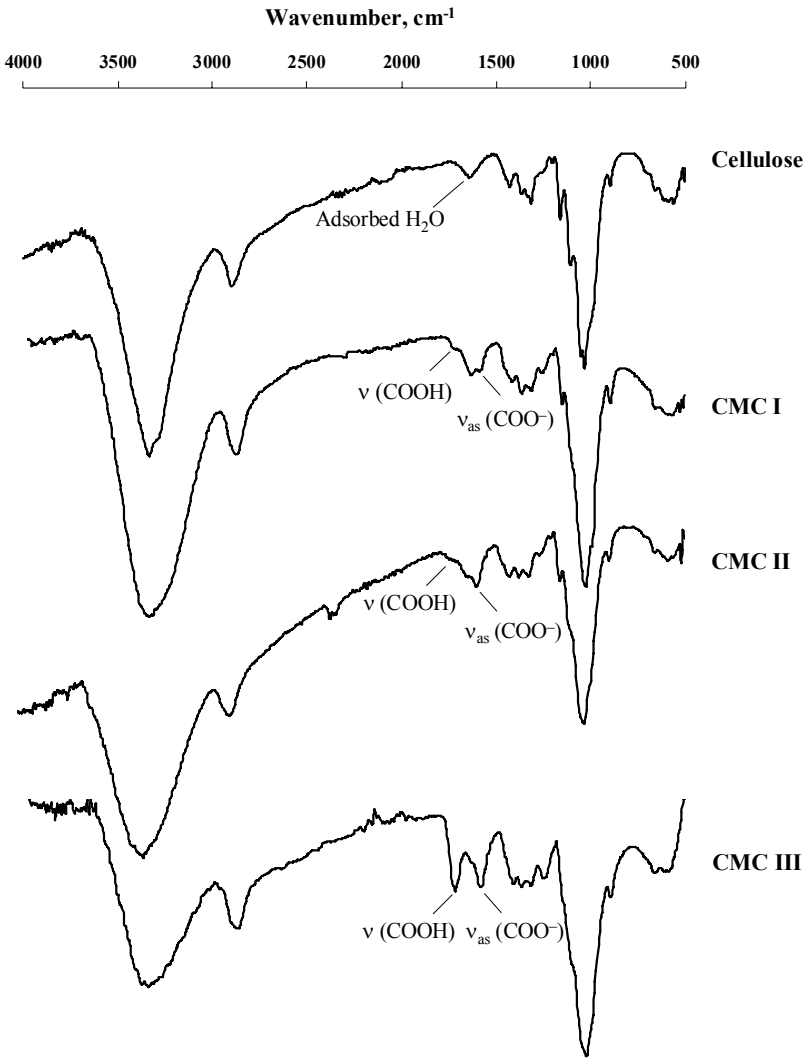

Figure 19: FTIR-ATR spectra of cellulose fibres before and after carboxymethylation (See Table 1 for CMC identification).

The comparison of these FTIR-ATR spectra allowed to confirm that in the case of CMC I and CMC II only a limited fraction of the total hydroxyl groups had reacted, because no substantial

changes in the intensity of the –OH stretching absorption band (3200 –3400 cm^{-1}) were observed. In the case of CMC III, the lower intensity of –OH stretching absorption band together with higher intensity of the characteristic absorption bands of carboxyl groups showed that the amount of carboxyl groups introduced in the fibres and the fraction of the total hydroxyl groups that react were very high. These results were in agreement with the carboxyl content determined by the back titration method (Figure 17) where CMC III had the highest carboxyl content and CMC I the lowest one.

1.3 X-Ray Diffraction

X-Ray diffraction is a powerful tool extensively used for the investigation of the cristallinity of cellulose fibres and their derivatives. The cellulose fibres of *Eucalyptus globulus* ECF bleached kraft pulp showed the typical XRD pattern of cellulose I [26]. The main diffraction peaks occur at around 2θ = 14.9º, 16.3º, 22.5º and 34.6º which are usually assigned to the diffraction planes 101, $10\bar{1}$, 002, and 040, respectively [26]. The diffractograms of CMC fibres correspond essentially to the XRD pattern of amorphous cellulose [26]. This means that the carboxymethylation reaction occurred on both amorphous and crystalline regions of the cellulose chains leading to the partial destruction of the crystalline supramolecular structure of cellulose. As an example, Figure 20 illustrates the X-ray diffractograms of cellulose and CMC I.

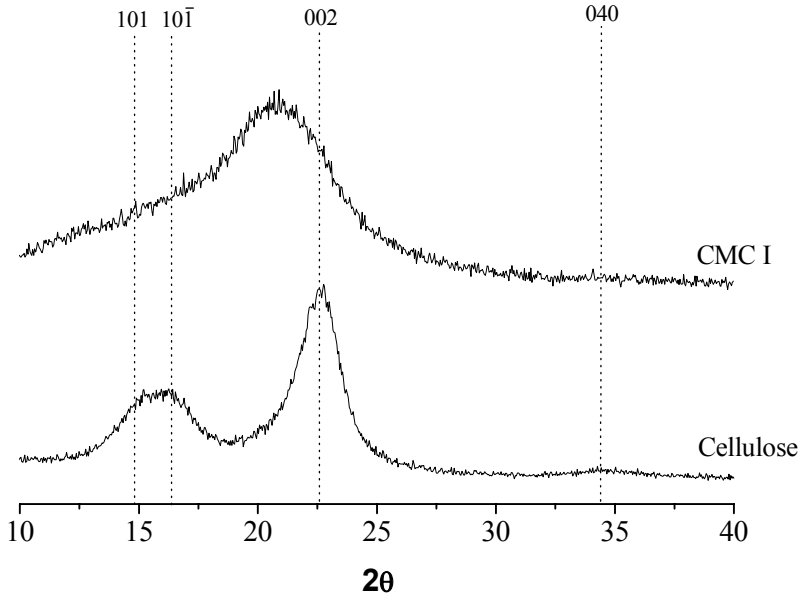

Figure 20: X-ray diffractograms of cellulose and CMC I fibres (See Table 1 for CMC identification).

1.4 Thermal degradation

The thermal decomposition behaviour of a sample can be investigated by thermal analysis techniques like thermogravimetry analysis (TGA). This technique is extensively employed to measure weight or mass changes as a function of temperature.

Typical TGA curves for cellulose fibres as well as carboxymethylcellulose fibres are presented in Figure 21. The thermal degradation profile of cellulose fibres followed a single-step reaction with a maximum decomposition temperature around 376°C. In general, carboxymethylated cellulose fibres present a lower thermal stability than the initial fibres since they start to decompose at temperatures considerably lower. This behaviour is related with the decrease in crystallinity associated with the destruction of the supramolecular structure of cellulose by the carboxymethylation reaction.

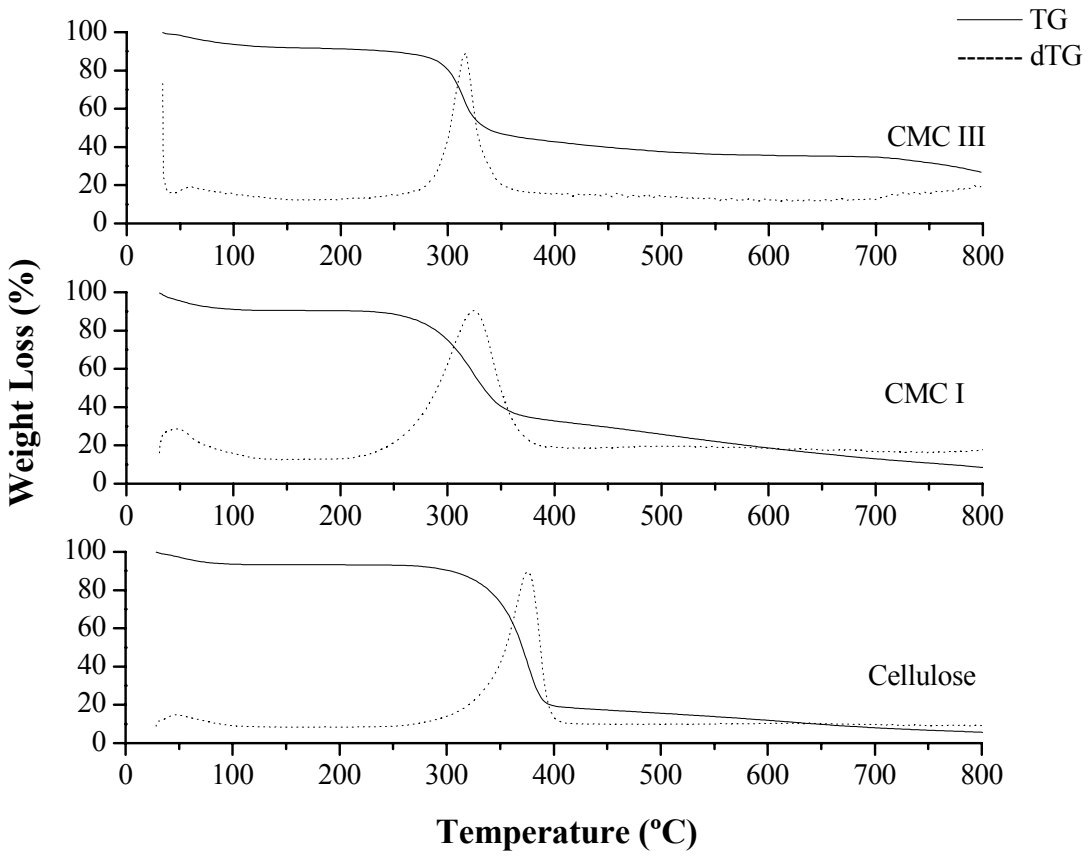

Figure 21: Thermograms of unmodified and modified cellulose fibres (See Table 1 for CMC identification).

The thermal decomposition temperatures of modified fibres ranged from 317°C for CMC III (carboxyl content of 1.83 mmol/g) to 325°C for CMC I (carboxyl content of 0.49 mmol/g). This means that the thermal stability of carboxymethylcellulose decreased with the increasing carboxyl content (Figure 21). The thermograms also showed that CMC III had a high inorganic residue (~27%) which was a consequence of the higher content of sodium on carboxylate groups, as shown in the IR spectra of CMC III (Figure 19).

1.5 Scanning Electron Microscopy

The morphology of the unmodified and modified cellulose fibres was evaluated by scanning electron microscopy (SEM). According to the micrographs, considerable changes in the fibrous morphology were observed before and after carboxymethylation. Figure 22 shows typical SEM micrographs of cellulose (carboxyl content: 0.10 mmol/g), and CMC II (carboxyl content: 0.83 mmol/g) fibres. The surface roughness of the CMC fibres is also different when compared to the pristine cellulose fibres. A plausible explanation for this phenomenon might be related with the formation of a gel-like material during the modification reaction due to the affinity of carboxyl groups toward water molecules. At the end of the carboxymethylation the gel-like material is washed with ethanol and the fibres regain their fibrous shape although with some dissimilarities.

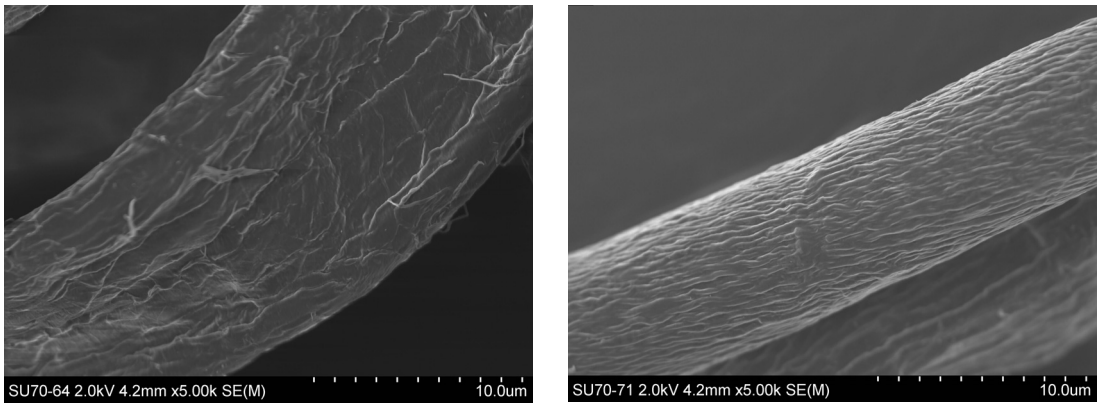

Cellulose **CMC II**

Figure 22: SEM micrographs of pristine cellulose fibres and carboxymethylated cellulose fibres (See Table 1 for CMC II identification).

1.6 Concluding Remarks

Hardwood bleached kraft pulp and carboxymethylated fibres were the two type of cellulose substrates used in this study. They were analysed for carboxyl content and characterized by IR, XRD, TGA and SEM.

The main features of cellulose fibres of hardwood bleached kraft pulp are their carboxyl content of 0.10 mmol/g and, as expected, the XRD pattern of cellulose I. In turn, the main characteristics of carboxymethylated fibres are a carboxyl content between 0.49-1.83 mmol/g, the XRD pattern of amorphous cellulose, different surface roughness and a thermal stability lower than that of cellulose.

2 SYNTHESIS AND CHARACTERIZATION OF CELLULOSE/ $CaCO_3$ NANOCOMPOSITES

The deposition of calcium carbonate on the surface of the cellulose fibres was done using an environmentally friendly route based on the $CaCl_2 – H_2O – (CH_3O)_2CO$ system. After the addition of calcium chloride and dimethylcarbonate to an aqueous suspension of fibres, NaOH was added to the reacting suspension and the precipitation of $CaCO_3$ took place as a result of the release of carbon dioxide by the base-catalyzed hydrolysis of DMC:

$$(CH_3O)_2CO_{(l)} + 2OH^-_{(aq)} \longrightarrow 2CH_3OH_{(l)} + CO_3^{2-}{}_{(aq)} \quad \textbf{(Reaction 4)}$$

$$Ca^{2+}_{(aq)} + CO_3^{2-}{}_{(aq)} \longrightarrow CaCO_{3\,(s)} \quad \textbf{(Reaction 5)}$$

In order to optimize the experimental conditions of the precipitation reaction of calcium carbonate at the surface of the fibres, a series of cellulose/$CaCO_3$ nanocomposites were prepared under distinct experimental conditions as summarized in Table 2. The effect of several reaction parameters, such as reaction time, temperature, fibre quantity, and the extent of the cellulose modification, on the final characteristics of the nanocomposites was investigated by ICP-AES, IR, XRD, SEM and TGA. It is worth mentioning that the influence of the cellulose modification on the deposition of $CaCO_3$ on the surface of the fibres could not be evaluated for CMC III (carboxyl content: 1.83 mmol/g). In fact, it was not possible to remove the nanocomposite from the reaction mixture by filtration. This occurrence might be due to the affinity of carboxyl groups toward water molecules which led to the formation of a gel-like material. The high viscosity of carboxymethylcellulose (CMC III) due to a high quantity of carboxyl groups did not allowed the filtration since it blocked the pores of all kind of filter paper grade.

Subsequent to the optimization of the experimental conditions, a large scale production of nanocomposite was carried out in order to prepare larger amounts of cellulose/$CaCO_3$ nanocomposites for the preparation of PE-cellulose/$CaCO_3$ composites. The nanocomposites prepared under scale-up conditions (nanocomposite N and O, Table 2) were used for ToF-SIMS and XPS studies.

2.1 Effect of reaction conditions

2.1.1 Inductively Coupled Plasma-Atomic Emission Spectrometry

The weight percentages of calcium deposited on the cellulose fibres were determined by inductively coupled plasma-atomic emission spectrometry (ICP-AES) and are shown in Figure 23. The ICP results gave a first glance over the effect of the studied reaction parameters on the final characteristics of the nanocomposites.

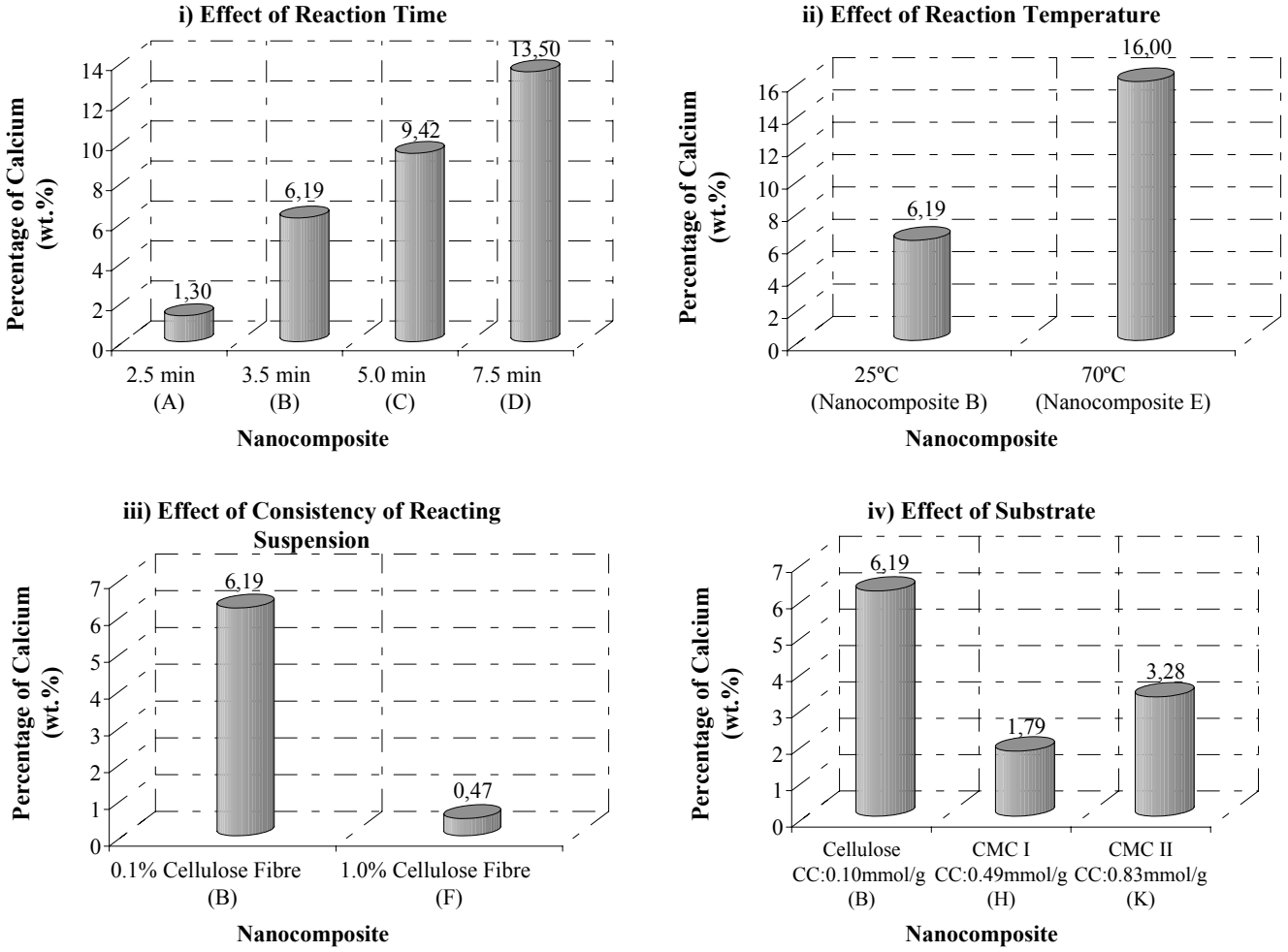

Figure 23: Effect of some reaction parameters on the percentage of calcium deposited on the fibres (See Table 2 for nanocomposite identification).

According to the results presented in Figure 23 the quantity of Ca^{2+} present in the cellulose fibres increased with increasing reaction times (Figure 23i, comparison between nanocomposites A, B, C and D). Besides, higher temperatures originated higher percentages of $CaCO_3$ (Figure 23ii, comparison between nanocomposites B and E). Additionally, higher consistencies of the reacting suspensions resulted as expected in much lower percentages of deposited calcium carbonate (Figure 23iii, comparison between nanocomposites B and F). Finally, against our expectations, the amount of $CaCO_3$ particles precipitated on the presence of cellulose is higher than on the presence of carboxymethylcellulose (Figure 23iv, comparison between B, H and K). As later will be shown by the subsequent analysis, this situation can be explained by the fact that CMC fibres promote the control growth of $CaCO_3$ particles and avoid their precipitation on the bulk of the solution. Ultimately, the percentage of Ca is higher for CMC II (carboxyl content = 0.83 mmol/g) than for CMC I (carboxyl content = 0.49 mmol/g). This indicates that higher carboxyl contents promote the precipitation of calcium carbonate particles, as already reported by other researchers [18].

2.1.2 Infrared Spectroscopy

The study of the IR spectra of the unmodified and modified cellulose/$CaCO_3$ nanocomposites showed that all the nanocomposites preserved the typical absorption bands of the cellulose backbone (Figure 18). Moreover, the IR spectra provided confirmation of the precipitation of calcium carbonate in the presence of cellulose fibres. This is evident by the presence of the absorption bands of $CaCO_3$: strong intensity band at 1420 cm^{-1} and medium intensity band at 876 cm^{-1}, which are characteristic of calcite the most stable polymorph of $CaCO_3$ [107]. As an example, Figure 24 presents the IR spectra of composites B, D, E, F, H and K.

The IR results were all in agreement with the ICP-AES results, except in the case of nanocomposite E. As shown in Figure 24, the IR results for nanocomposite E ruled out the presence of calcium carbonate since there was no absorption bands assigned to this inorganic compound. Nevertheless, the high percentage of calcium ions present in nanocomposite E (Figure 23) is attributable to calcium hydroxide, as will be shown by the XRD data (Part III, Section 2.1.3).

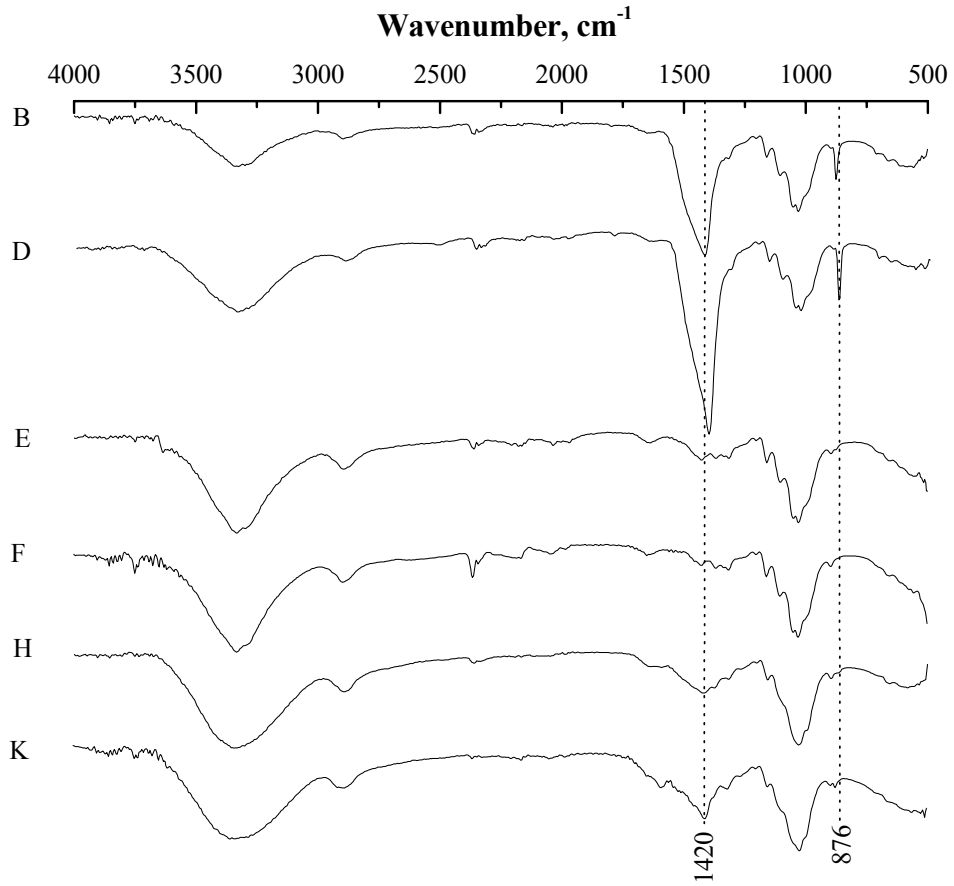

Figure 24: FTIR-ATR spectra of nanocomposites B, D, E, F, H and K (See Table 2 for nanocomposites identification).

2.1.3 X-Ray Diffraction

The nanocomposites of cellulose/$CaCO_3$ were characterized by XRD to evaluate the effect of the type and quantity of reinforcement on the cristallinity of cellulose fibres and polymorphism of calcium carbonate. The characteristic peaks of $CaCO_3$ polymorphs are evident at:

(i) calcite: 2θ = 23.2º, 29.5º, 36.0º, 39.3º, 43.0º, 48.4º [46,66];

(ii) aragonite: 2θ = 26.5º, 45.9º, 50.1º [46,108];

(iii) vaterite: 2θ = 21.0º, 25.0º, 27.0º, 32.7º [109].

All the nanocomposites preserved the XRD pattern of the corresponding substrate, suggesting that the deposition of $CaCO_3$ did not affect the structure of the cellulose or CMC fibres. As an example, Figure 25 shows the XRD patterns of nanocomposites B, D, E, F, H and K (See Table 2 for nanocomposite identification). As it may be seen from the diffractograms, the nanocomposites produced at a reaction time of 3.5 min (nanocomposite B) are formed by a mixture of two polymorphic phases of calcium carbonate: calcite and vaterite. The nanocomposites produced at a reaction time of 7.5 min (nanocomposite D) contain mainly calcite and some traces of vaterite in the cellulosic matrix. This clearly points to the transformation of the unstable vaterite into the most thermodynamically stable calcite with time. Some works have shown that the crystallization of $CaCO_3$ polymorphs is a rather complicated process, composed of the competitive nucleation and crystal growth of the polymorphs, and the phase transformation from metastable to stable forms [47,49,107].

The nanocomposites obtained at 70°C (nanocomposite E) exhibited several characteristic diffraction peaks of calcium hydroxide at 2θ = 18.0°, 28.7° and 34.1° [66]. The presence of $Ca(OH)_2$ also explains the FTIR spectra (Figure 24) of this sample, where the $CaCO_3$ characteristic bands were not observed. The non-occurrence of the precipitation of calcium carbonate at 70°C might be related with the evaporation of dimethylcarbonate, whose boiling point range is 86-89°C, and subsequent no release of CO_2 by the base-catalysed hydrolysis of dimethylcarbonate. As a result, $Ca(OH)_2$ precipitated by the reaction of calcium chloride with sodium hydroxide:

$$CaCl_2 + 2NaOH \rightarrow Ca(OH)_2 + 2NaCl \qquad \textbf{(Reaction 6)}$$

The XRD pattern of nanocomposite F shows no distinguished diffraction peaks which might mean that the quantity of calcium carbonate deposited onto the substrate was at a level below the detection limit of this technique. Nevertheless, this small quantity of $CaCO_3$ is in agreement with the ICP-AES and IR data.

When the carboxyl content of the substrate is raised up to 0.49 mmol/g (nanocomposite H) there is also no diffraction peaks characteristic of the polymorphic phases of $CaCO_3$. So, the amount of $CaCO_3$ must be below the detection limit of the XRD technique. However, a superior carboxyl content (0.83 mmol/g – nanocomposite K) originated a single diffraction peak characteristic of calcite 2θ = 29.5° [66]. This indicates that higher contents of carboxyl groups promote the precipitation of calcite.

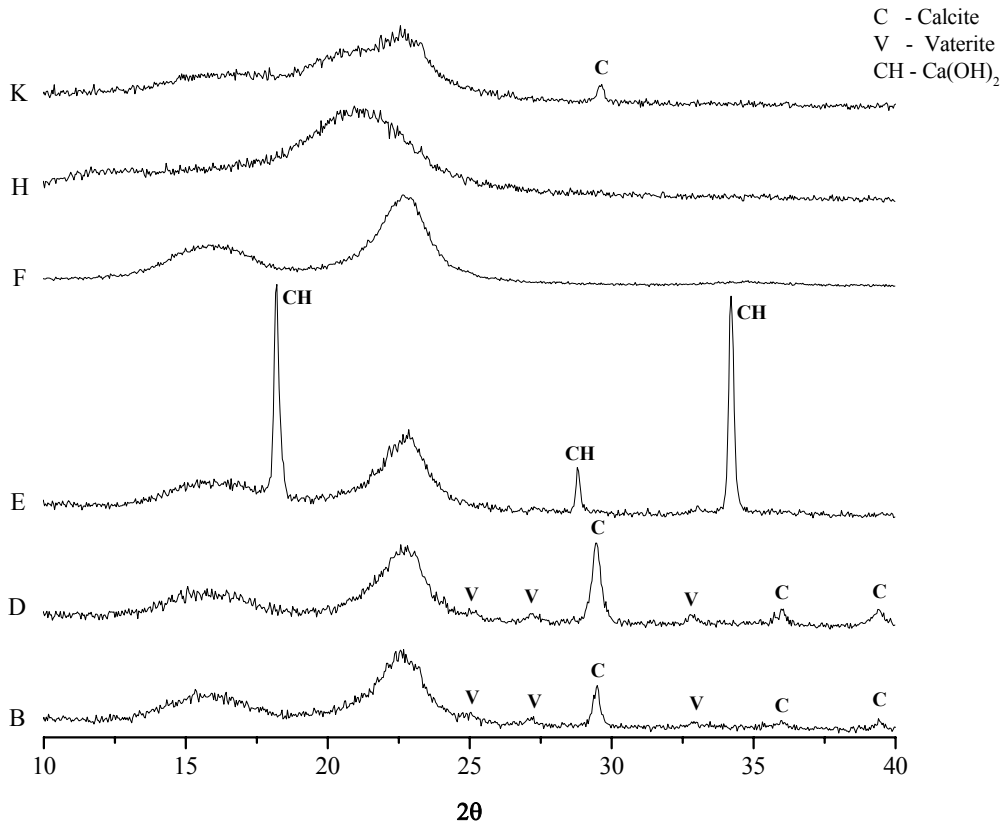

Figure 25: X-ray diffractogram of nanocomposites B, D, E, F, H and K (See Table 2 for nanocomposites identification).

In order to draw a conclusion regarding the effect of the in situ synthesis of $CaCO_3$ particles in the presence of cellulose fibres, a sample of $CaCO_3$ particles were precipitated by the DMC method at 25ºC for 3.5 minutes in the absence of the fibres. The powder XRD diffractogram of the inorganic particles is shown in Figure 31. All the diffraction peaks were assigned to calcite, the most stable polymorph of calcium carbonate. This suggests that the presence of cellulosic fibres during the precipitation of calcium carbonate influenced its polymorphic form, as may be seen by comparing the diffractograms of $CaCO_3$ (Figure 26) and nanocomposites B and F (Figure 25).

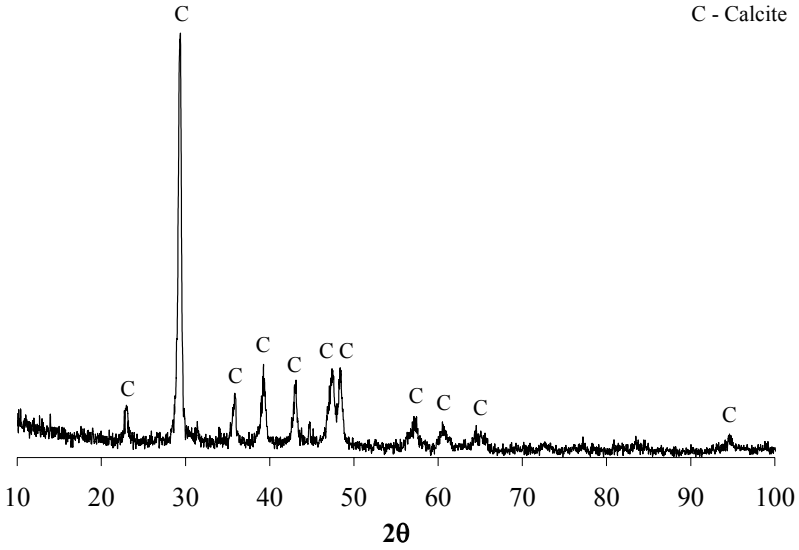

Figure 26: X-ray diffractogram of calcium carbonate.

2.1.4 Scanning Electron Microscopy

The calcium carbonate deposition into cellulose fibres was monitored by SEM. The morphological development of the $CaCO_3$ particles was followed at different reaction times and temperatures, consistencies of the reacting suspensions and carboxyl contents of the substrates. All the previous parameters influenced the $CaCO_3$ particle size and morphology. The $CaCO_3$ particle size ranged between 200 and 700 nm, while the morphologies were spherical for almost every nanocomposite.

As an example, Figure 27 shows SEM micrographs of nanocomposites B, D, E, F, H and K. The comparison between nanocomposites B and D showed that increasing the reaction time from 3.5 to 7.5 minutes substantially increased the amount and size of $CaCO_3$ deposited on the cellulose fibres. In addition, the SEM micrograph of nanocomposite B shows that at 25^{o}C, nanosized (ca. 400 nm) calcium carbonate particles with spheroidal morphology were produced. However, temperature obviously influenced the chemical composition of the inorganic particles since at 70^{o}C (nanocomposite E), micrometric aggregates of a calcium compound ($Ca(OH)_2$) were obtained. When the consistency of the reacting suspensions was increased from 0.1% (nanocomposite B) to 1.0% (nanocomposite F) the amount and size of $CaCO_3$ deposited on the fibres diminished, although the morphology of the particles remained spherical. The chemical modification of the cellulosic substrate from cellulose (nanocomposite B) to carboxymethylcellulose (nanocomposites

H and K) originated smaller $CaCO_3$ particles (ca. 200 nm). The presence of carboxyl groups at the cellulose surface seemed to promote the control growth of $CaCO_3$ on the surface of cellulose fibres.

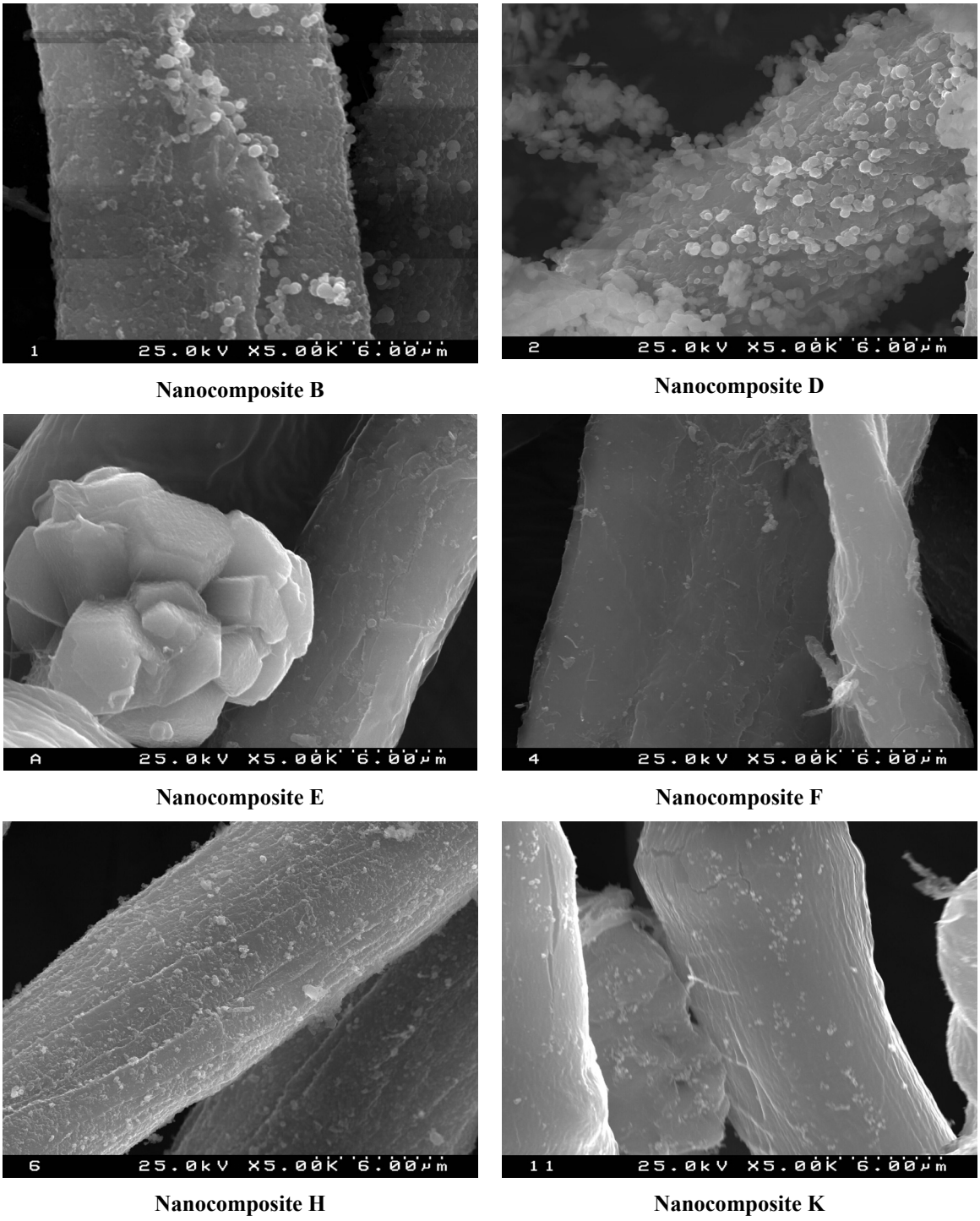

Nanocomposite B **Nanocomposite D**

Nanocomposite E **Nanocomposite F**

Nanocomposite H **Nanocomposite K**

Figure 27: SEM micrographs of nanocomposites B, D, E, F, H and K (See Table 2 for nanocomposites identification).

It is noteworthy that when the substrate is unmodified cellulose fibres with 0.1% of consistency of the reacting suspension, there is a considerable amount of $CaCO_3$ particles that did not adhered to the surface of the fibres. That is to say that a higher quantity of $CaCO_3$ in the nanocomposites doesn't mean that the inorganic particles were all attached into the surface of cellulose fibres. This is completely evident in the case of nanocomposite D (Figure 27). However, when higher consistencies of the reacting suspension (1.0%) were used (nanocomposite F) the precipitation of $CaCO_3$ on the bulk of the solution was reduced. Additionally, the use of carboxymethylated cellulose fibres as the substrate also avoids the precipitation of calcium carbonate on the bulk of the solution since it improves the selectivity of precipitation on fibres.

Ultimately, it is important to refer that the presence of fibres during the precipitation of calcium carbonate particles influenced their morphology and aggregation degree. Figure 28 clearly indicates that $CaCO_3$ particles precipitated by the DMC method at 25ºC for 3.5 minutes in the absence of cellulosic fibres exhibit irregular nano-sized (200-500 nm) aggregate particles.

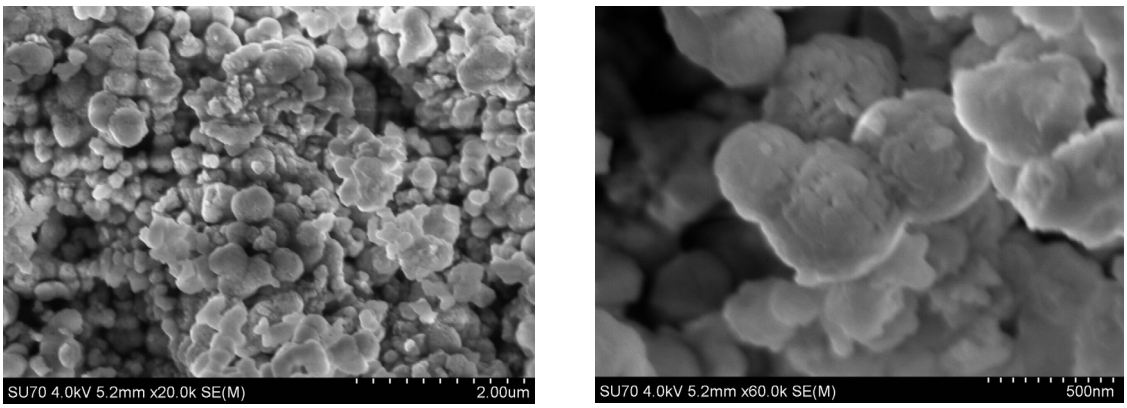

Figure 28: SEM micrographs of calcium carbonate particles at different magnifications.

2.1.5 Thermal degradation

Thermal gravimetric analysis was used to check the thermal behaviour of the nanocomposites of cellulosic fibres and calcium carbonate. It is important to bear in mind that the thermal degradation profile of cellulose fibres followed a single-step reaction with a maximum decomposition temperature around 376ºC, while CMC fibres presented a lower thermal stability than the initial fibres with lower decomposition temperatures. Additionally, the thermal degradation profile of calcium carbonate can be roughly divided into three mass loss steps. The first two steps in the range of 20-180ºC and with a total mass loss of about 10% might be attributed

to the evaporation of the physically and chemically adsorbed water. The third step (600-765ºC), where the largest mass loss was observed (33%), could be assigned to the thermal decomposition of $CaCO_3$ to calcium oxide and carbon dioxide ($CaCO_{3\,(s)} \rightarrow CaO_{\,(s)} + CO_{2\,(g)}$). The thermal behaviour of this $CaCO_3$ sample prepared at 25ºC for 3.5 minutes in the absence of cellulosic fibres (Figure 29 and Figure 30) is in good agreement with literature [110,111].

On the whole, the deposition of calcium carbonate into the surface of the fibres originated less stable materials since they started to decompose at temperatures considerably lower than the original fibres. This suggests that the incorporation of inorganic particles into the surface of the fibres did not improve the thermal stability of the ensuing materials, at least within the experimental conditions in which we worked. A possible explanation for this phenomenon may be the fact that the fibres suffered a minor degradation during the in situ deposition of $CaCO_3$ on the substrates due to swelling in water.

As an example, the TGA curves of $CaCO_3$, nanocomposites B, D, E, F and cellulose are shown in Figure 29, while the TGA curves of CMC I, $CaCO_3$ and nanocomposites H and K are illustrated in Figure 30. It is worth mentioning that when carboxymethylcellulose is used as the substrate the thermal behaviour of the corresponding nanocomposites was quite similar to the modified fibres, while in the case of cellulose the difference between the thermal decomposition temperature of the fibres and the resultant nanocomposites was significant, as may be seen in Figure 29 and Figure 30. For instance, the maximum decomposition temperature was around 376ºC for cellulose, 332ºC for nanocomposite B and 328ºC for nanocomposite F whereas the maximum decomposition temperature was 325ºC for CMC I and 327ºC for nanocomposite H.

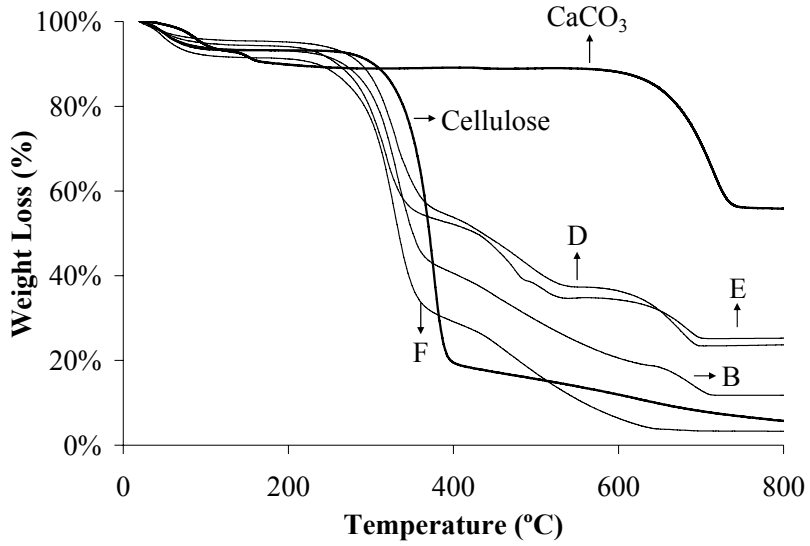

Figure 29: Thermograms of $CaCO_3$, cellulose and nanocomposites B, D, E and F (See Table 2 for nanocomposites identification).

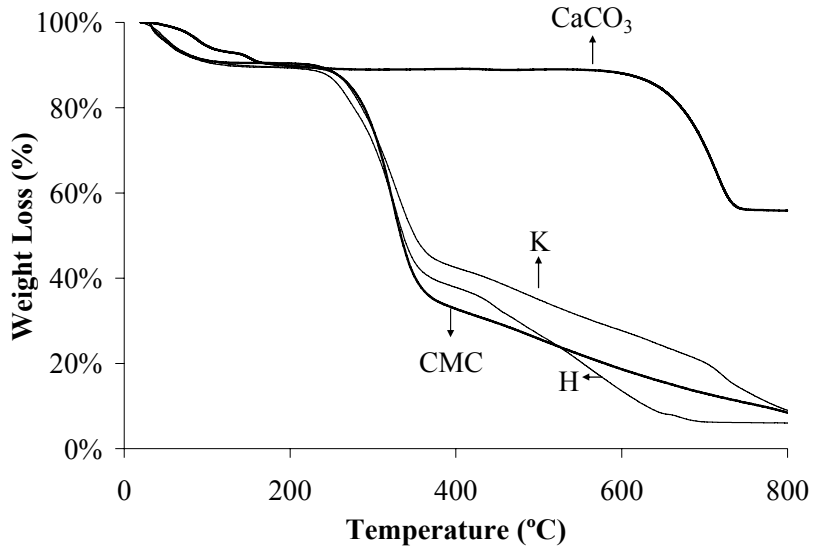

Figure 30: Thermograms of $CaCO_3$, CMC I and nanocomposites H and K (See Table 1 and Table 2 for CMC and nanocomposites identification, respectively).

2.1.6 Time-of-flight Secondary Ion Mass Spectrometry

Time-of-flight secondary ion mass spectrometry (ToF-SIMS) is an analytical technique used to study the detailed surface chemical composition. The ToF-SIMS spectra of the kraft pulp and carboxymethylated fibres are shown in Figure 31, while Figure 32 shows the ToF-SIMS spectra of nanocomposites N and O (see Table 2 for nanocomposite identification).

The *Eucalyptus globulus* ECF bleached kraft pulp fibres (cellulose) and the carboxymethylated fibres (CMC I) showed characteristic fragments assigned to cellulose (127 and 145 Da) and hemicelluloses, e.g. xylans, (115 and 133 Da) [112]. The absence of the typical peaks of hardwood lignin (137, 151, 167, 181 Da) [112,113] pointed out that the pulping and bleaching processes were efficient in the removal and/or chemical degradation of lignin. Secondary ion peaks attributable to Na, Al and Ca (23, 27 and 40 Da, respectively) were also observed at low mass regions. Moreover, in the higher mass regions, several peaks normally assigned to wood extractives (free fatty acid, fatty acid salts and sterols) [114] were also identified.

The ToF-SIMS surface characterization of the nanocomposites N and O clearly confirmed the success of the deposition of calcium carbonate on the fibres surface, since the intensity of the Ca peak visibly increases (Figure 32). This intensity was higher for nanocomposite O than for nanocomposite N which corroborates the ICP-AES and IR data. Obviously the secondary ions attributed to cellulose, xylans, other metal ions and extractives were also detected in the ToF-SIMS spectra of nanocomposites N and O.

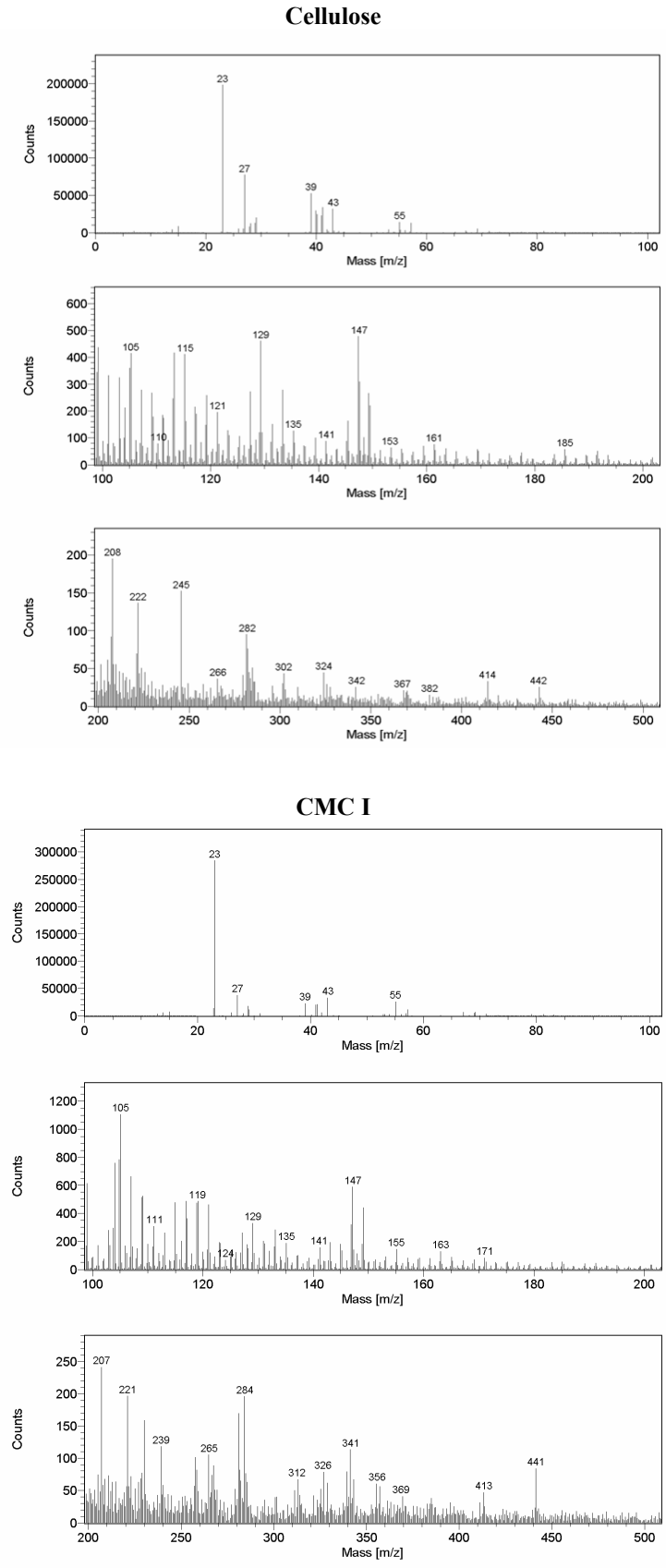

Figure 31: ToF-SIMS spectra (positive mode) of cellulose and CMC I (See Table 1 for CMC identification).

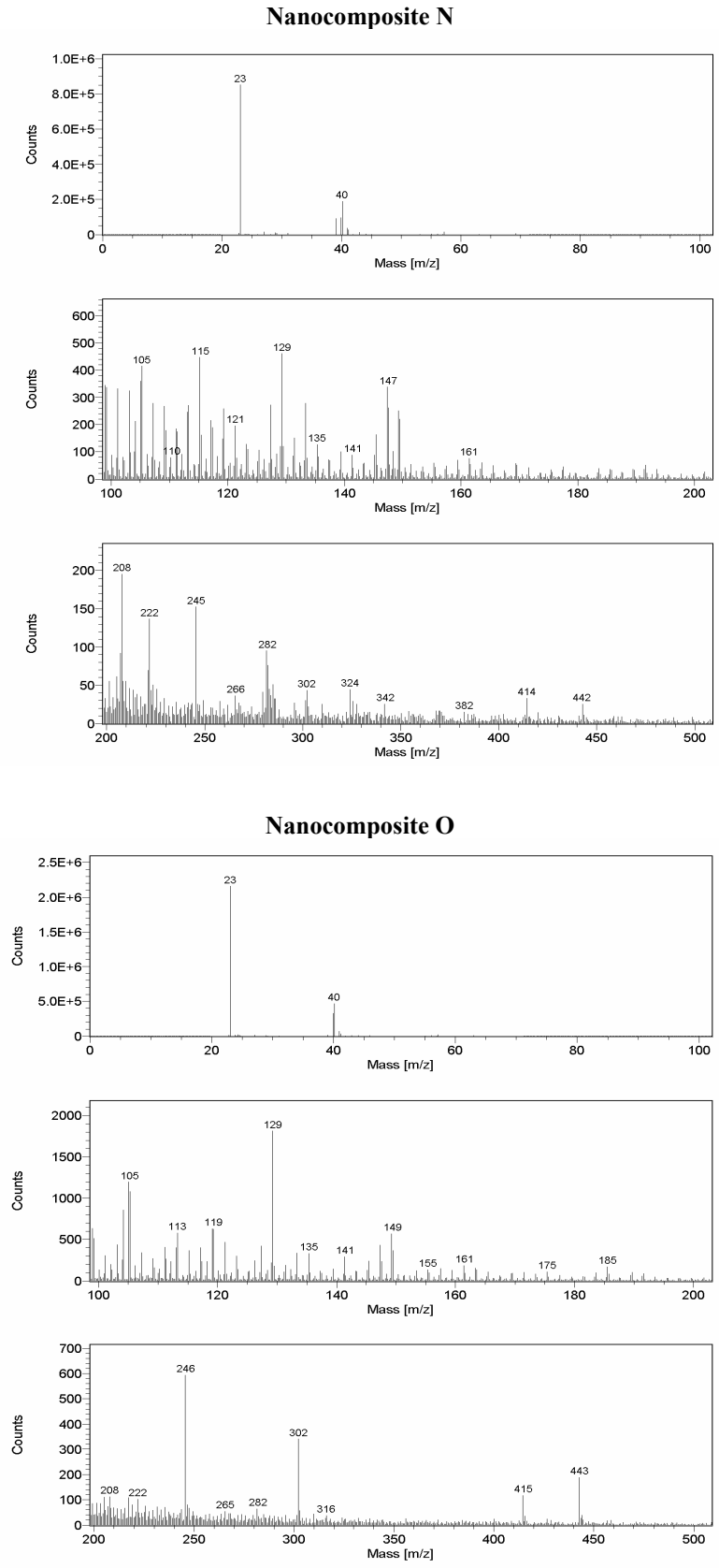

Figure 32: ToF-SIMS spectra (positive mode) of nanocomposites N and O (See Table 2 for nanocomposites identification).

Additionally, ToF-SIMS imaging was employed to assess the distribution of calcium carbonate attached onto the fibres' surface by monitoring the calcium ions. The images in positive mode of total and Ca ion of nanocomposites N (cellulose/$CaCO_3$) and O (CMC I/$CaCO_3$) are shown in Figure 33. It was observed that the distribution of calcium carbonate onto the fibres surface is quite heterogeneous, particularly for the unmodified fibres where some agglomeration spots can be observed. These results also indicate that the presence of carboxyl moieties play an important role on the $CaCO_3$ precipitation.

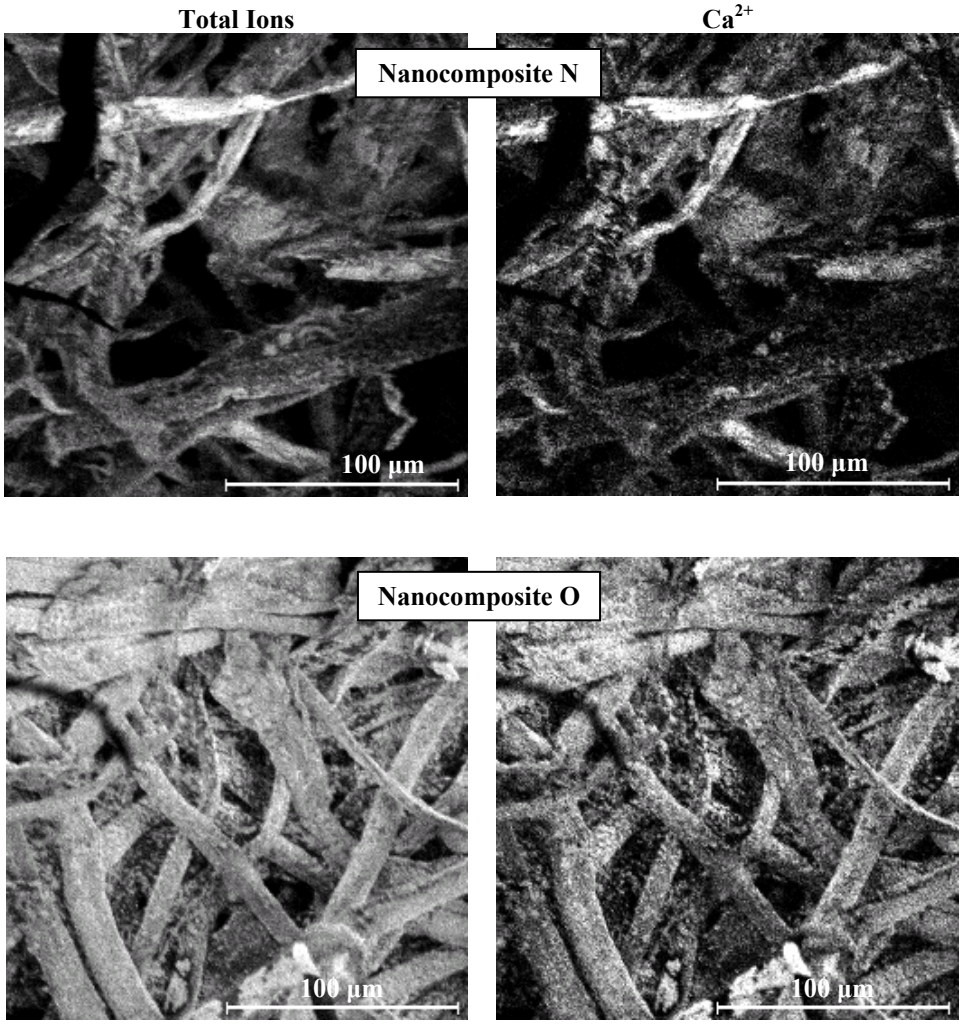

Figure 33: ToF-SIMS imaging of nanocomposites N and O showing the distribution of calcium ions attached onto the fibres' surface (See Table 2 for nanocomposites identification).

2.1.7 X-Ray Photoelectron Spectroscopy

X-Ray photoelectron spectroscopy (XPS) can be used as a direct probe of the surface composition profile. This surface characterization technique analyses the photoelectrons emitted from the core levels in atoms [115]. The chemical composition of cellulose, carboxymethylcellulose, and nanocomposites N and O was analysed using low- and high-resolution XPS.

The low-resolution XPS spectra are displayed on Figure 34 and Figure 35 and the elements (C, O, Ca) compositions are summarized in Table 3. At low-resolution C1s (~285eV) and O1s (~533eV) [116] were dominant elements detected in all samples. The presence of $CaCO_3$ in the nanocomposites was evidenced by the emergence of a peak (Ca2p) at a binding energy of around 350 eV which is characteristic of calcium [117]. Finally, the detection of small amounts of other elements like Na and Cl on the surface of nanocomposites was related with their ineffective washing during the synthesis procedure.

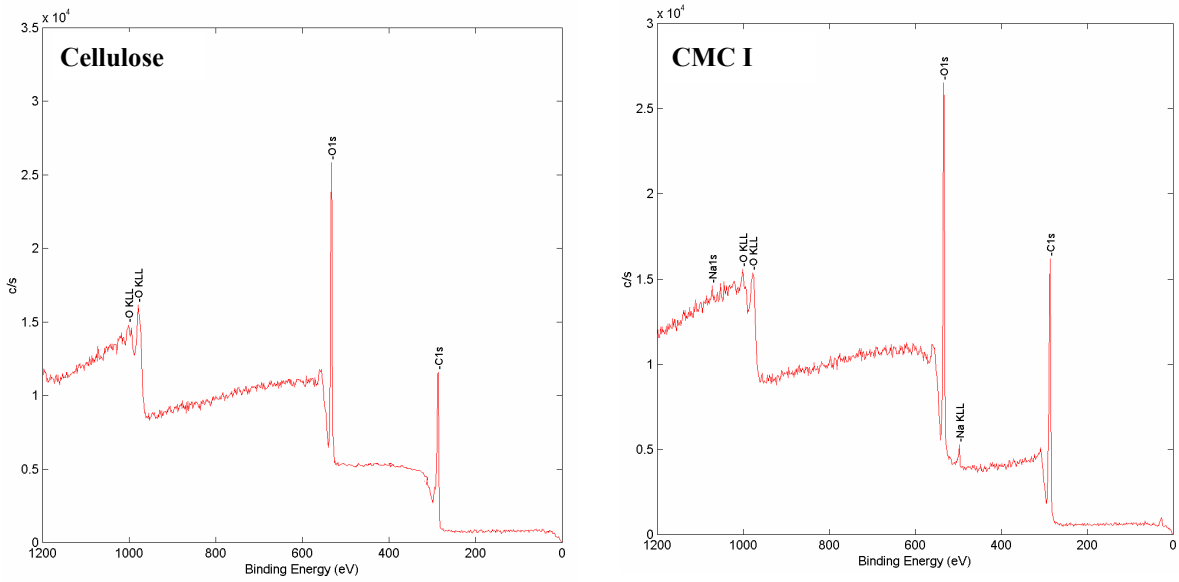

Figure 34: Low resolution XPS spectra of cellulose and CMC I (See Table 1 for CMC identification).

It is noteworthy that the percentage of calcium present at the surface of nanocomposite N (cellulose/$CaCO_3$) is lower than at the surface of nanocomposite O (CMC/$CaCO_3$) – Table 3. This corroborates the SEM observations which indicate that carboxymethylated fibres enhance the selectivity of precipitation on the surface of the fibre, avoiding the precipitation on the bulk of the

solution. However, the percentages of calcium obtained by ICP are lower when compared to the values obtained by low-resolution XPS. These differences arise from the fact that ICP determines the percentage of calcium in the entire sample while XPS determines the percentage of calcium only at the surface of the sample.

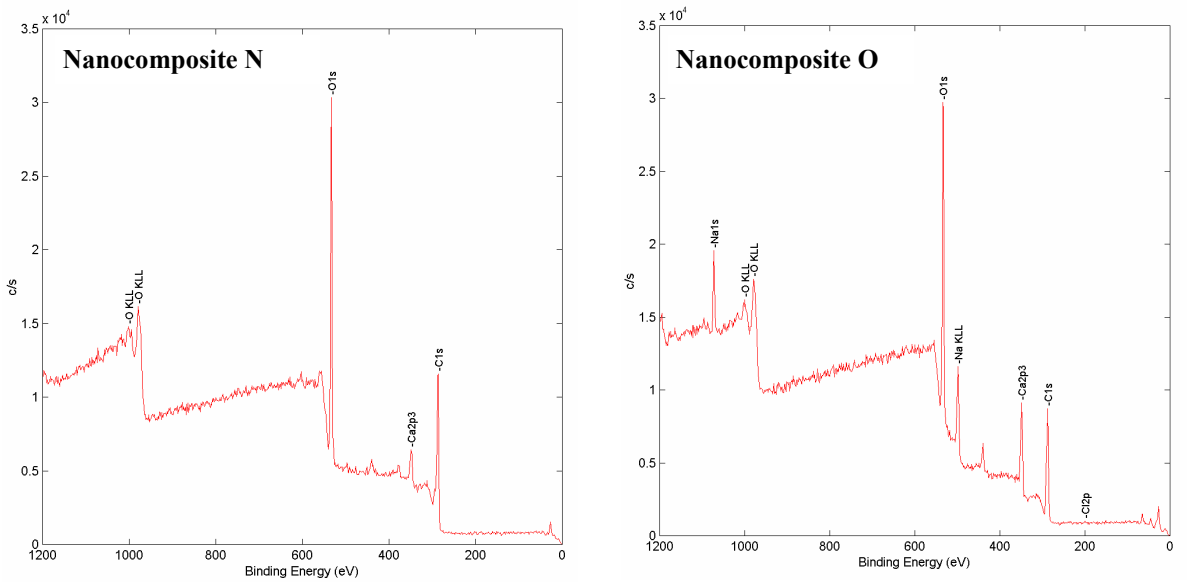

Figure 35: Low resolution XPS spectra of nanocomposites N and O (See Table 2 for nanocomposites identification).

Table 3: Low-resolution XPS results of cellulose, CMC I, and nanocomposites N and O

Sample*	O (%)	C (%)	O/C	Ca (%)	Na (%)	Cl (%)
Cellulose	42.9	57.1	0.75	–	–	–
Nanocomposite N	42.5	55.1	0.77	2.3	–	0.1
CMC I	35.2	64.2	0.55	–	0.7	–
Nanocomposite O	37.9	51.2	0.74	5.1	5.6	0.2

* See Table 1 and Table 2 to identify the samples.

Depending on the local environment, atoms of the same element emit electrons from the same core level with different binding energies [115]. This feature referred to as chemical shifts might result from differences in: molecular environment, oxidation states, location in a crystal lattice, etc [115]. Figure 36 and Figure 37 shows the high-resolution XPS survey spectra of the substrates and nanocomposites, where it is possible to see the peak deconvolutions of the C1s signals. The peak areas are compiled in Table 4.

The high-resolution deconvolution of the C1s peak of cellulose resulted in four distinct peaks, as shown in Figure 36. These four deconvoluted peaks correspond to the four chemical environments of carbon: C1 (C–C, C–H), C2 (C–O), C3 (O–C–O or C=O), and C4 (O=C–O) [115]. The C1 peak has a binding energy of 285.0 eV and is used as the reference of binding energy. So, the binding energies, relative to C1 position, for the other three chemical environments of carbon are: 1.5 eV for C2, 3.0 eV for C3 and 4.0-5.0 eV for C4 [115,116].

High-resolution deconvolution of the C1s peak of CMC I (Figure 36) revealed that the carboxymethylation reaction (–CH_2COOH) of cellulose really occurred since the peak areas of the carbons in a hydrocarbon environment (C1) and in a carboxyl moiety (C4) increased, as displayed in Table 4.

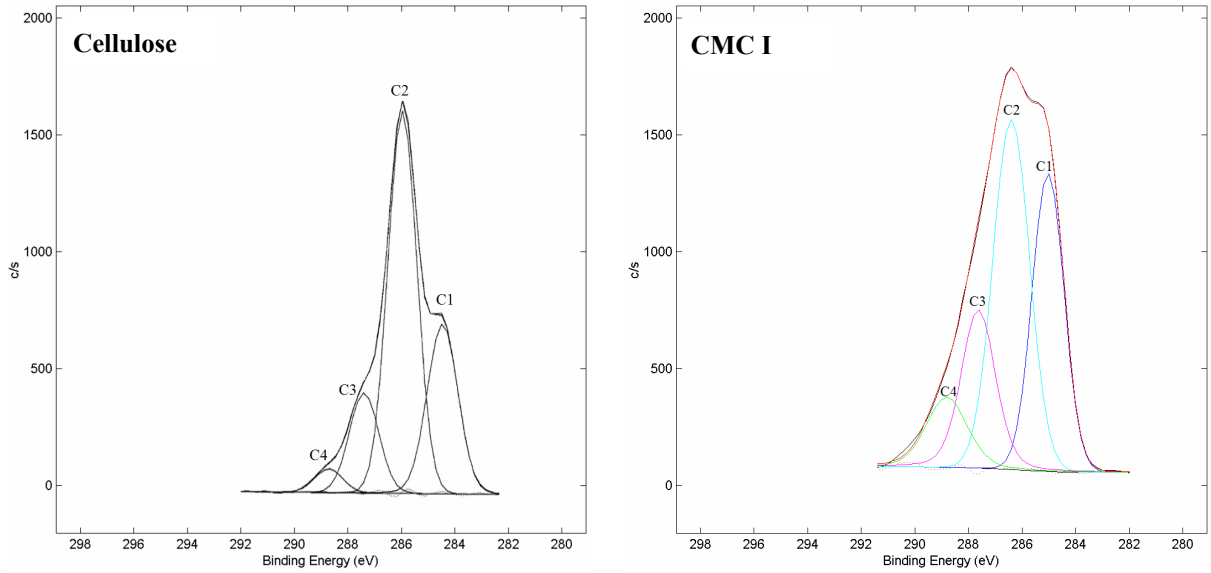

Figure 36: XPS high-resolution spectra of cellulose and CMC I (See Table 1 for CMC identification).

The presence of $CaCO_3$ in the nanocomposites was confirmed in the high-resolution XPS (Figure 37 and Table 4) by the emergence of a peak at around 290 eV due to the carbonate carbon atom (CO_3^{2-}) [118,119]. The curve fitting of C1s of nanocomposite N identified C1, C2, C3, C4, and three carbon environments with the binding energies of 5.6 ± 0.3 eV for C5, 8.6 ± 0.3 eV for C6 and 10.6 ± 0.3 eV for C7 relative to the C1 position. The C5 position was assigned to CO_3^{2-} while the C6 and C7 positions might be shake-up or plasmon structures rather than emission lines of photoelectron [115,116,120]. The high-resolution deconvolution of nanocomposite O revealed C1, C2, C3, C4, and the carbon environment (C5) at around 290 eV assigned to carbonate. According to the data in Figure 37 and Table 4, the $CaCO_3$ content was higher in nanocomposite O

than in nanocomposite N. These results were in agreement with the ICP-AES, IR and ToF-SIMS data.

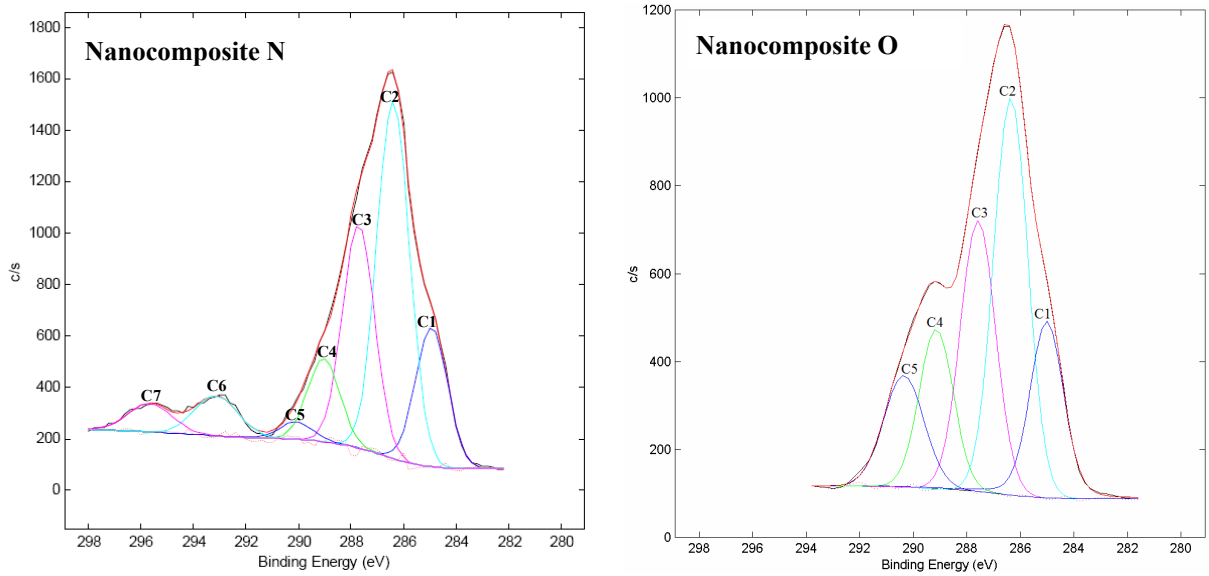

Figure 37: XPS high-resolution spectra of nanocomposites N and O (See Table 2 for nanocomposites identification).

Table 4: High-resolution XPS results of cellulose, CMC I, and nanocomposites N and O

Sample*	Peak area (%)						
	C1 (C–C; C–H)	C2 (C–O)	C3 (O–C–O; C=O)	C4 (O–C=O)	C5 (CO_3^{2-})	C6	C7
Cellulose	22.0	61.7	13.0	3.3	–	–	–
Nanocomposite N	15.2	39.3	24.5	9.1	1.9	5.9	4.2
CMC I	28.4	40.9	19.0	11.7	–	–	–
Nanocomposite O	15.5	35.1	24.8	13.3	11.4	–	–

* See Table 1and Table 2 to identify the samples.

2.2 Concluding Remarks

The hydrolysis of dimethylcarbonate in alkaline medium is an effective, reproducible and a straightforward chemical route to precipitate and grow $CaCO_3$ particles at the surface of cellulosic substrates. In addition, the quantity and morphology of $CaCO_3$ particles deposited at the surface of the cellulose fibres were strongly dependent on the hydrolysis conditions:

(i) the amount and size of $CaCO_3$ deposited on the cellulose fibres increased with increasing reaction time;

(ii) the reactions performed at room temperature originated nanosized $CaCO_3$ particles with spheroid morphology, while at 70°C micrometric aggregates of $Ca(OH)_2$ were obtained;

(iii) lower consistencies of the reacting suspensions favoured the formation of spheroid particles;

(iv) the presence of carboxyl groups at the cellulose surface promoted the selective control growth of $CaCO_3$ on the surface of the fibres.

The results provided by the combined use of ToF-SIMS and XPS confirmed the presence of calcium carbonate particles at the surface of the cellulosic fibres and corroborated all the results of the other analysis.

The precise mechanism by which $CaCO_3$ is retained in the cellulosic fibres remains an issue that should be further investigated in a near future.

3 POLYETHYLENE-CELLULOSE/$CaCO_3$ COMPOSITES

In this chapter the preparation of polyethylene (PE) based composites with cellulose/$CaCO_3$ nanocomposites as the reinforcing phase is described in detail. The PE-based composites were prepared by mixing the polymer with different fillers (cellulose and nanocomposite N, Figure 38) and different filler contents (0, 15 and 30%), as summarized in Table 5. The properties of the PE-based composites were assessed by SEM, DSC and DMA.

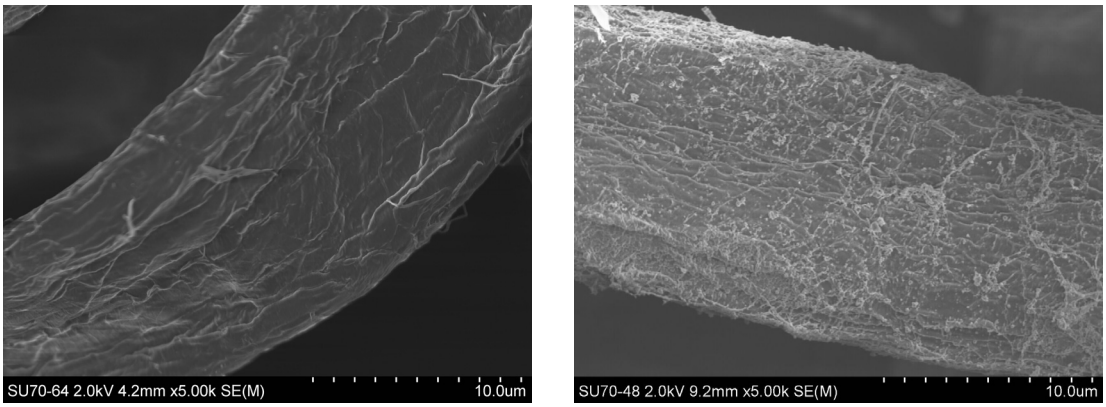

Cellulose **Nanocomposite N**

Figure 38: SEM micrographs of cellulose and nanocomposite N (See Table 2 for nanocomposite identification).

Table 5: Compositions of the PE-based composites

Sample identification	Matrix (wt.%)	Compatibilizer (wt.%)	Filler (wt.%)	
	PE	PE-*g*-MA	Cellulose	Cellulose/$CaCO_3$ (Nanocomposite N)
PE	100	0	0	0
PE-1	85	0	15	0
PE-2	70	0	30	0
PE-3	85	0	0	15
PE-4	70	0	0	30
PE-5	83	2	15	0
PE-6	68	2	30	0
PE-7	83	2	0	15
PE-8	68	2	0	30

A relevant observation regarding these materials is that the colour of the different composites slightly changed from white to dark yellow with the incorporation of different reinforcements, as may be seen in Figure 39. The darker colours indicate thermal degradation probably as a result of the compounding temperature of the composites (170ºC), and the in situ deposition of $CaCO_3$ on the substrate (Part III, section 2.1.5), which originated lesser thermal stable materials.

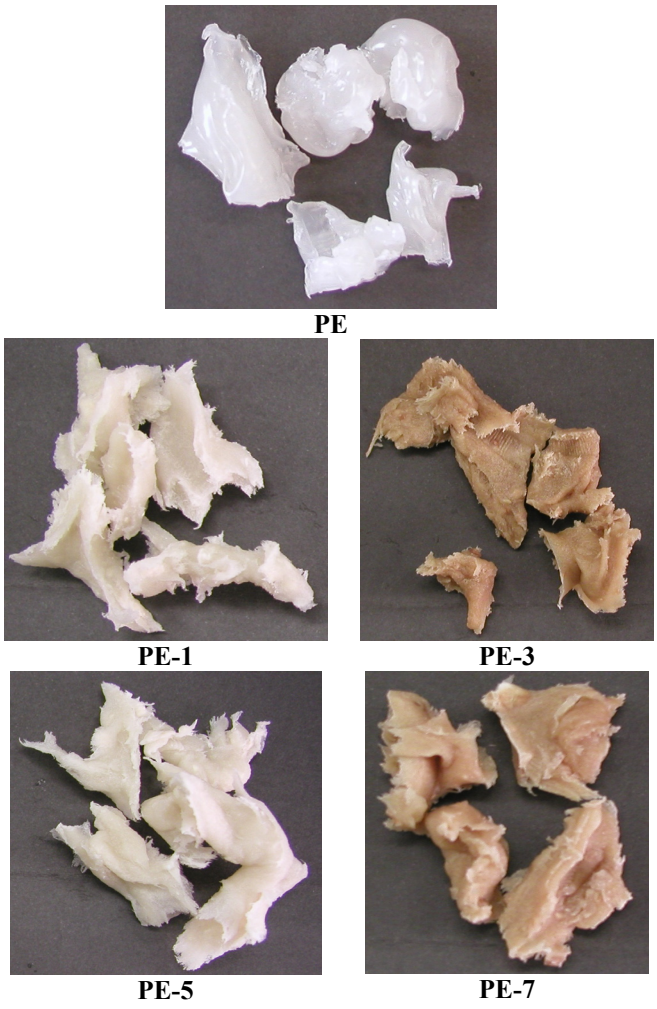

Figure 39: Photographs of PE and its composites (See Table 5 for PE composites identification).

3.1 Scanning Electron Microscopy

Scanning electron micrographs of the fracture surfaces of the different polyethylene based composites were performed to observe the morphology and the filler/matrix interactions. In a general overview, the fractured surface of PE-based composites shows that the dispersion of the

reinforcements (cellulose and nanocomposite N) in the matrix is rather heterogeneous. Nevertheless, the fibres appeared to remain undamaged suggesting that the applied mechanical shear in the blender did not result in fibre fracture.

As an example, Figure 40 illustrates the microstructures of fractured surfaces of PE-1, PE-3, PE-6 and PE-8 and is possible to see that the majority of the reinforcements (cellulose and nanocomposite N) are exposed and dispersed unevenly. Not even the use of a compatibilizing agent, which had been reported to improve the interfacial adhesion with the matrix [100], reduced the exposure and increased the dispersion of the reinforcing nanocomposite.

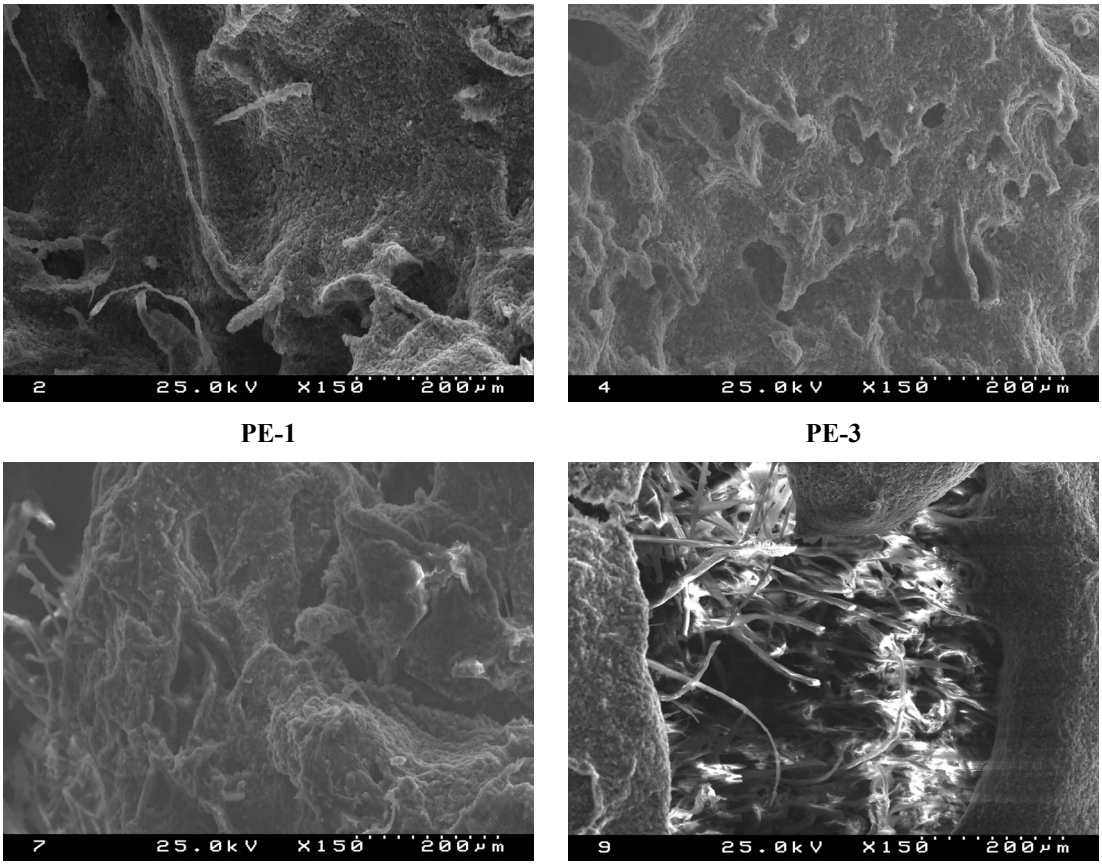

PE-1 **PE-3**

PE-6 **PE-8**

Figure 40: SEM micrographs of the fracture surface of PE-based composites (See Table 5 for PE composites identification).

3.2 Differential Scanning Calorimetry

The melting behaviour of polyethylene and derived composites was analysed by differential scanning calorimetry (DSC). Nine samples (PE, PE-1, PE-2, PE-3, PE-4, PE-5, PE-6, PE-7, PE-8)

were tested to evaluate how the addition of different contents of cellulose fibres and nanocomposite N (cellulose/$CaCO_3$) with and without a compatibilizer would affect the thermal behaviour of polyethylene. Figure 41 shows the DSC curves of polyethylene (PE) and composites PE-1, PE-2, PE-3 and PE-4, while Figure 42 displays the DSC curves of polyethylene (PE), compatibilizing agent (polyethylene-*graft*-maleic anhydride (PE-*g*-MA)) and composites PE-5, PE-6, PE-7 and PE-8. The melting characteristics and the degree of crystallinity of PE and its composites are summarized in Table 6.

The DSC data shows that the melting temperature (T_m) of polyethylene (113ºC) is comparable to the one given by the manufacturer (116ºC, Part II, Section 1.1) and is in the typical melting range for low-density polyethylene (LDPE) [121]. Besides, the crystallinity degree of PE, determined by DSC as 33% (Table 6), is also in conformity with literature [101,104].

The incorporation of cellulose fibres and nanocomposite N into PE had no significant effect on the melting behaviour of this polymer, as can be seen in the melting curves of PE-1, PE-2, PE-3 and PE-4 composites. The little fluctuation of T_m observed is within the typical experimental accuracy for this kind of measurements [122].

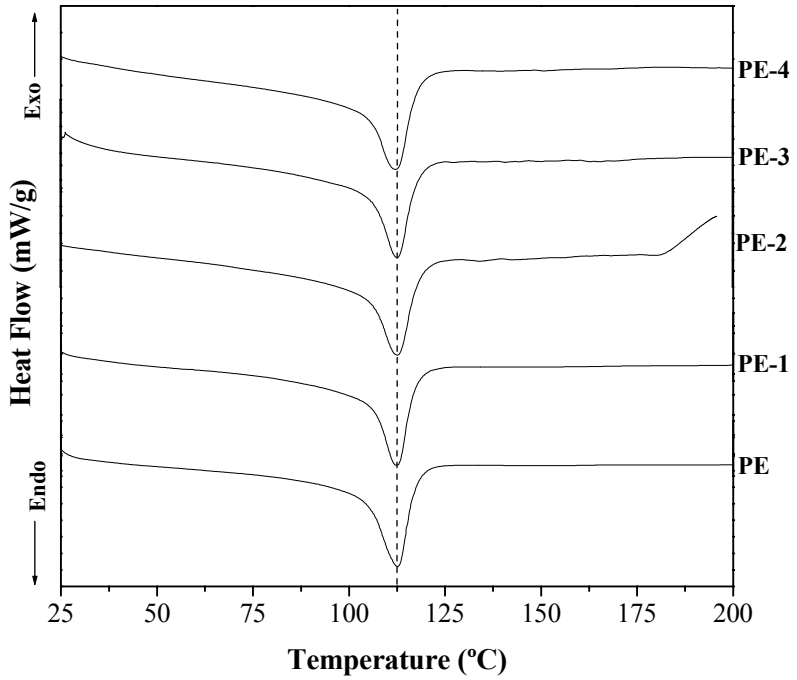

Figure 41: Melting behaviour of PE, PE-1, PE-2, PE-3 and PE-4 as determined by DSC (See Table 5 for PE composites identification).

On the other hand, the incorporation of cellulose and nanocomposite N into PE together with a compatibilizing agent (PE-*g*-MA) slightly influenced the melting temperature of this thermoplastic. According to Figure 42 and Table 6, the T_m of polyethylene slightly decreased with the use of a compatibilizer, except in the case of composite PE-8 where T_m suffered a small increase from 113 to 114ºC. Still, the fluctuations in the melting temperature were so small that we might consider that the melting behaviour of PE wasn't affected by the use of 2% of a compatibilizing agent together with the reinforcing phase.

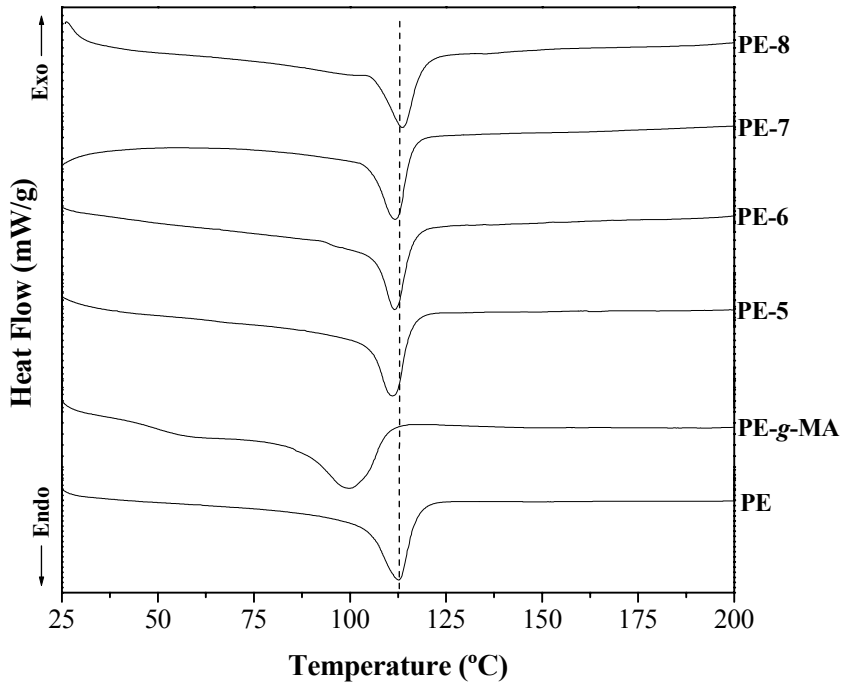

Figure 42: Melting behaviour of PE, PE-*g*-MA, PE-5, PE-6, PE-7 and PE-8 as determined by DSC (See Table 5 for PE composites identification).

Finally, the crystallinity of PE was not considerably affected by the use of cellulose and cellulose/$CaCO_3$ as reinforcing element (Table 6).

Table 6: Melting characteristics and degree of crystallinity of PE and its composites assessed by DSC

Samples*	T_m (^oC)	ΔH_m (J/g) [a]	X_c (%) [a]
PE	113	98	33
PE-1	113	94	32
PE-2	113	102	35
PE-3	113	95	33
PE-4	112	100	34
PE-5	111	95	32
PE-6	112	101	34
PE-7	112	96	33
PE-8	114	100	34

* See Table 5 for PE composites identification; [a] For 100% polymer (PE).

3.3 Dynamic Mechanical Analysis

Dynamic mechanical analysis (DMA) provides information about the mechanical and viscoelastic properties as a function of temperature through the application of an oscillating force. The DMA of the PE based composites was performed to investigate if the addition of different fillers (cellulose and composite N) would influence the mechanical behaviour of PE.

Representative curves of the storage modulus (E') of PE and its composites are shown in Figure 43 and Figure 44. As can be seen, the storage modulus (Figure 43) of PE and PE-based composites decreased monotonically with the increase in temperature. The incorporation of cellulose or cellulose/$CaCO_3$ as filler in the polyethylene matrix has significant effect on the storage modulus (elastic properties). According to Figure 43, the E' increased with increasing amount of filler and, for a given percentage of filler, the use of cellulose/$CaCO_3$ instead of cellulose originated higher values of storage modulus. At room temperature, for example, the modulus of the composites increased from 150 MPa for neat PE up to 255 MPa for PE-1 (15 wt.% cellulose), 289 MPa for PE-3 (15 wt.% cellulose/$CaCO_3$), 531 MPa for PE-2 (30 wt.% cellulose) and 380 MPa for PE-4 (30 wt.% cellulose/$CaCO_3$). The discrepancy in the value of E' of PE-2 might be related with the presence of agglomerates of fibres in the composite.

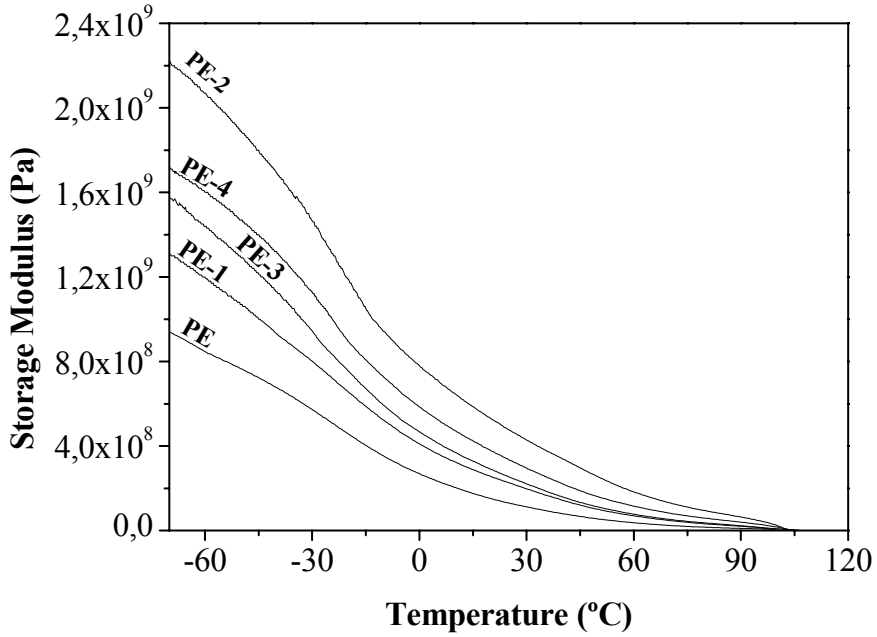

Figure 43: The dynamic storage modulus curves of PE, PE-1, PE-2, PE-3 and PE-4 (See Table 5 for PE composites identification).

In the compatibilized PE composites (Figure 44), the behaviour is similar to that mentioned for the uncompatibilized composites (Figure 43). For instance, at room temperature the modulus of the composites increased from 150 MPa for neat PE up to 264 MPa for PE-5 (15 wt.% cellulose), 271 MPa for PE-7 (15 wt.% cellulose/$CaCO_3$), 395 MPa for PE-6 (30 wt.% cellulose) and 408 MPa for PE-8 (30 wt.% cellulose/$CaCO_3$). The comparison between composites with and without compatibilizer shows that the effect of PE-g-MA was not significant in the improvement of the fibre/PE interactions, at least for the weight percentage that was used. These results were in agreement with the DSC analysis.

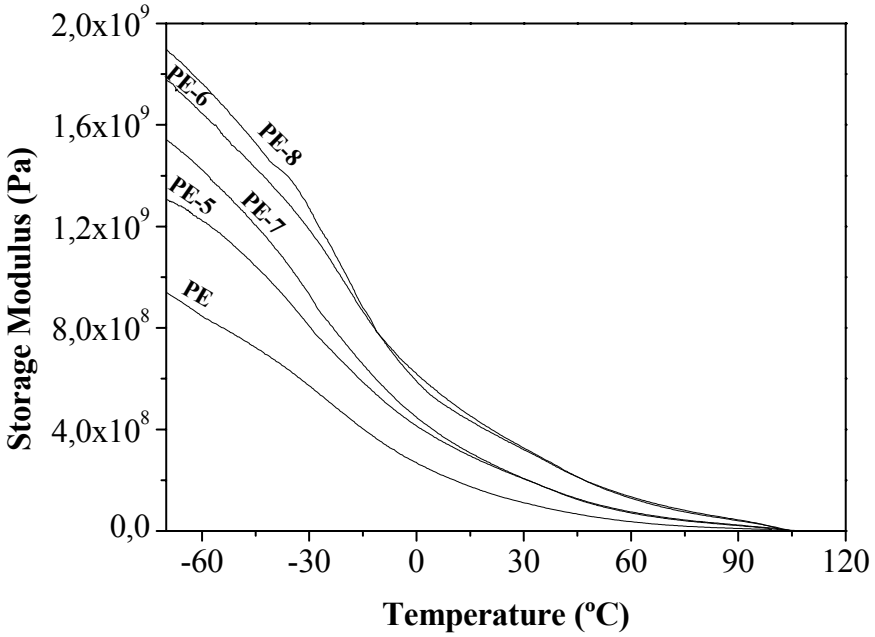

Figure 44: The dynamic storage modulus curves of PE, PE-5, PE-6, PE-7 and PE-8 (See Table 5 for PE composites identification).

3.4 Concluding Remarks

Polymer matrix composites of polyethylene were one of the potential applications for cellulose/$CaCO_3$ materials. The incorporation of cellulose/$CaCO_3$ nanocomposites into low density polyethylene did not influenced the melting behaviour neither the crystallinity degree of PE. In turn, it demonstrated reinforcement effects that contributed to the increase of the storage modulus of the material.

As a result of the tendency of cellulose fibres to form aggregates with non polar polymers during processing, the use of a compatibilizing agent was necessary to improve fibre/matrix interactions. However, the PE-g-MA did not show any compatibilizing effect on PE-cellulose/$CaCO_3$ composites. It is possible that the amount of PE-g-MA added was not enough to show its compatibilizing effect.

PART IV – CONCLUSIONS AND FUTURE WORK

The main goal of this study was to produce cellulose/$CaCO_3$ nanocomposites by a simple and environmentally friendly route, and to investigate potential applications.

The nanocomposites were synthesized by a method based on the generation of carbon dioxide from an organic precursor (DMC). The effect of several reaction parameters (reaction time and temperature, fibre quantity and extent of cellulose modification) on characteristics of the ensuing materials was evaluated by different techniques. The first conclusion to be drawn was that the hydrolysis conditions strongly influenced the quantity and morphology of $CaCO_3$ particles deposited at the surface of cellulose fibres. Moreover:

(i) higher reaction time means higher quantity and size of $CaCO_3$ particles;

(ii) reactions carried out at room temperature originated nanosized $CaCO_3$ particles (calcite/vaterite) with spheroid morphology, while at 70^{o}C micrometric aggregates of $Ca(OH)_2$ were obtained;

(iii) lower consistencies of the reacting suspensions favoured the formation of spheroid particles of $CaCO_3$;

(iv) the presence of carboxyl groups at the substrate surface increases the selectivity of precipitation of calcite on the surface of the fibre.

The mechanism by which $CaCO_3$ particles are retained at the surface of cellulosic fibres is not understood at this stage, thus it remains an issue that should be further investigated.

PE-based composites were one of the possible applications for cellulose/$CaCO_3$ nanocomposites. Despite the poor dispersion of the filler (cellulose/$CaCO_3$ nanocomposites) in the polyethylene matrix, the DMA results were encouraging. This analysis showed that the use of cellulose/$CaCO_3$ nanocomposites as reinforcing agent originated PE composites with higher storage modulus than the corresponding PE composites with cellulose as reinforcement. This indicates that the presence of $CaCO_3$ particles improved the stiffness of PE-based composites.

FUTURE WORK

In a near future, other issues concerning potential applications of cellulose fibre/$CaCO_3$ nanocomposites should be carried on. One of the most promising applications for the prepared nanocomposites might be polymer matrix composites, albeit the difficulty to achieve well dispersed reinforcements in the polymer matrix. Nevertheless, the performance of the composites might be improved by adding compatibilizers to enhance the interaction between the matrix and reinforcements, functionalizing the reinforcement or adding nano-sized reinforcements [76].

Polyethylene based composites have already been studied here as a potential application for cellulose/$CaCO_3$ nanocomposites. Although the results were positive, the performance of the PE-based composites should be improved by finding a suitable medium to separate the cellulose fibres together with the use of a feeding medium which do not cause degradation of the fibres or the polymer in high processing temperatures. Moreover, the effect of the addition of compatibilizers to enhance the interaction between the matrix (PE) and reinforcements should be further evaluated.

Besides PE, other polymers like poly(lactic acid) (PLA) can also be used as matrix. This polyester of lactic acid ($HOCH_3CHCOOH$), mainly obtained from renewable agricultural raw materials which are fermented to lactic acid [123], is one of the most promising biodegradable polymers. The main features of this versatile polymer are its good stiffness and strength, and its low toughness and thermal stability. PLA-based composites have been studied by several researchers with the aim of producing products were biodegradability is wanted [73,124]. To our knowledge practically no information is available on polymer based composite materials of PLA and cellulosic fibres/calcium carbonate.

REFERENCES

[1] Klemm, D.; Heublein, B.; Fink, H.-P.; Bohn, A.; *Cellulose: Fascinating Biopolymer and Sustainable Raw Material,* Angewandte Chemie 44, 3358-3393, 2005.

[2] Klemm, D.; Philipp, B.; Heinze, T.; Heinze, U.; Wagenknecht, W.; C*omprehensive Cellulose Chemistry*: *Fundamentals and Analytical Methods*, volume 1, Wiley-VCH: Verlag, 1998.

[3] John, M.J.; Thomas, S.; *Biofibres and biocomposites*, Carbohydrate Polymers 71, 343-364, 2008.

[4] Mohanty, A.K.; Misra, M.; Hinrichsen, G.; *Biofibres, biodegradable polymers and biocomposites: An overview,* Macromolecular Materials and Engineering 276/277, 1-24, 2000.

[5] Bledzki, A. K.; Gassan, J.; *Composites reinforced with cellulose based fibres*, Progress Polymer Science 24, 221-274, 1999.

[6] Eichhorn, S.J.; Baillie, C.A.; Zafeiropoulos, N.; Mwaikambo, L.Y.; Ansell, M.P.; Dufresne, A.; Entwistle, K.M.; Herrera-Franco, P.J.; Escamilla, G.C.; Groom, L.; Hughes, M.; Hill, C.; Rials, T.G.; Wild, P.M.; *Current International research into cellulosic fibres and composites*, Journal of Materials Science 36, 2107-2131, 2001.

[7] Sequeira, S.; Evtuguin, D. V.; Portugal, I.; Esculcas, A. P.; *Synthesis and characterization of cellulose/silica hybrids obtained by heteropoly acid catalysed sol-gel process,* Materials Science and Engineering C 27, 172-179, 2007.

[8] Pinto, R.J.B.; Marques, P.A.A.P; Barros-Timmons, A.M.; Trindade, T.; Pascoal Neto, C.; *Novel SiO_2/cellulose nanocomposites obtained by in situ synthesis and via polyelectrolytes assembly,* Composites Science and Technology 68, 1088-1093, 2008.

[9] Marques, P.A.A.P.; Trindade, T.; Pascoal Neto, C.; *Titanium dioxide/cellulose nanocomposites prepared by a controlled hydrolysis method,* Composites Science and Technology 66, 1038-1044, 2006.

[10] Pinto, R.J.B.; Marques, P.A.A.P; Martins, M.A.; Pascoal Neto, C.; Trindade, T.; *Electrostatic assembly and growth of gold nanoparticles in cellulosic fibres,* Journal of Colloid and Interface Science 312, 506-512, 2007.

[11] Fahmy, T.Y.A.; Mobarak, F.; *Nanocomposites from natural cellulose fibres filled with kaolin in presence of sucrose,* Carbohydrate Polymers 72, 751-755, 2008.

[12] Barata, M.A.B.; Neves, M.C.; Pascoal Neto, C.; Trindade, T.; *Growth of $BiVO_4$ particles in cellulosic fibres by in situ reaction*, Dyes and Pigments 65, 125-127, 2005.

[13] Feng, B.; Yong, A. K.; An, H.; *Effect of various factors on the particle size of calcium carbonate formed in a precipitation process*, Materials Science and Engineering A 445-446, 170-179, 2007.

[14] Fimbel, P.; Siffert, B.; *Interaction of calcium carbonate (calcite) with cellulose fibres in aqueous medium,* Colloids and Surfaces 20, 1-16, 1986.

[15] Dalas, E.; Klepetsanis, P. G.; Koutsoukos, P. G.; *Calcium Carbonate Deposition on Cellulose,* Journal of Colloid and Interface Science 224, 56-62, 2000.

[16] Subramanian, R.; Maloney, T.; Paulapuro, H.; *Calcium carbonate composite fillers*, Tappi Journal 4, 23-27, 2005.

[17] Isogai, A.; Kitaoka, C.; Onabe, F.; *Effects of carboxyl groups in pulp on retention of alkylketene dimmer*, Journal of Pulp and Paper Science 23, J215-J219, 1997.
Kiatoka, T.; Isogai, A.; Onabe, F.; *Chemical modification of pulp fibres by TEMPO-mediated oxidation,* Nordic Pulp and Paper Research Journal 14, 279-284, 1999.

[18] Dousi, E.; Kallitsis, J.; Chrissanthopoulos, A.; Mangood, A.H.; Dalas, E.; *Calcite overgrowth on carboxylated polymers*, Journal of Crystal Growth 253, 496-503, 2003.

[19] Hon, D. N.-S.; Shiraishi, N.; *Wood and Cellulosic Chemistry*, Marcel Dekker, New York, 1990.

[20] Krässig, H. A.; *Cellulose: structure, accessibility and reactivity*, Gordon and Breach Science Publishers, Switzerland, 1993.

[21] Sjöström, E.; *Wood Chemistry: Fundamentals and Applications*, Academic Press Inc. 2nd Edition, USA, 1993.

[22] O'Sullivan, A. C.; *Cellulose: the structure slowly unravels*, Cellulose 4, 173-207, 1997.

[23] Smook, G. A.; *Handbook for Pulp & Paper Technologists*, Angus Wilde Publications, 2nd Edition, 1997.

[24] Stage, C.; Granet, R.; Verneuil, B.; Branland, P.; Krausz, P.; *Synthesis and properties of biodegradable plastic films obtained by microwave-assisted cellulose acylation in homogeneous phase*, Comptes Rendus Chimie 7, 135-142, 2004.

[25] Zugenmaier, P.; *Conformation and packing of various crystalline cellulose fibers,* Progress in Polymer Science 26, 1341-1417, 2001.

[26] Metshitsuka, G.; Isogai, A.; *Chemical modification of lignocellulosic materials,* ed. D. N-S Hon. Marcel Dekker, 1996.

[27] Stenius, P.; *Papermaking Science and Technology*, ed. Per Stenius e Heikki Pakarinen. Fapet Oy. 3, 1999.

[28] Boluk, Y.; *Acid-base interactions and swelling of cellulose fibers in organic liquids*, Cellulose 12, 577-593, 2005.

[29] Klemm, D.; Heinze, T.; Philipp, B.; Wagenknecht, W.; *New approaches to advanced polymers by selective cellulose functionalization*, Acta Polymer 48, 277-297, 1997.

[30] Edgar, K.J.; Buchanan, C.M.; Debenham, J.S.; Rundquist, P.A.; Seiler, B.D.; Shelton, M.C.; Tindall, D.; *Advances in cellulose ester performance and application,* Progress in Polymer Science 26, 1605-1688, 2001.

[31] Heinze, T.; Liebert, T.; *Unconventional methods in cellulose functionalization,* Progress in Polymer Science 26, 1689-1762, 2001.

[32] Belgacem, M.N.; Gandini, A.; *Surface Modification of Cellulose Fibres,* Polímeros: Ciência e Tecnologia 15, 114-121, 2005.

[33] Heinze, T.; Liebert, T.; Klüfers, P.; Meister, F.; *Carboxymethylation of cellulose in unconventional media,* Cellulose 6, 153-165, 1999.

[34] Klemm, D.; Philipp, B.; Heinze, T.; Heinze, U.; Wagenknecht, W.; *Comprehensive Cellulose Chemistry*: *Functionalization of cellulose*, volume 2, Wiley-VCH: Verlag, 1998.

[35] Deer, W. A.; Howie, R. A.; Zussman, J.; *Introduction to the Rock Forming Minerals*, Longman: Harlow, UK, 1992.

[36] Dickens, B.; Bowen, J. S.; *Refinement of the crystal structure of the aragonite phase of* $CaCO_3$, Journal of Research of the National Bureau Standards, Section A: Physics and Chemistry 75, 27-32 ,1971.

[37] Richter, A.; Petzold, D.; Hofmann, H.; Ullrich, B.; *Production, properties and application of calcium carbonate powders Part I: production of calcium carbonate by precipitation from solutions*, Chemische Technik 6, 306-313, 1995.

[38] Zaremba, C.M.; Morse, D.E.; Mann, S.; Hansma, P.K.; Stucky, G.D.; *Aragonite-Hydroxyapatite Conversion in Gastropod (Abalone) Nacre*, Chemistry of Materials 10, 3813-3824, 1998.

[39] Xu, A.-W.; Antonietti, M.; Cölfen, H.; Fang, Y.-P.; *Uniform Hexagonal Plates of Vaterite* $CaCO_3$ *Mesocrystals Formed by Biommimetic Mineralization,* Advanced Functional Materials 16, 903-908, 2006.

[40] Aizenberg,J.; Lambert, G.; Weiner, S.; Addadi, L.; *Factors Involved in the Formation of Amorphous and Crystalline Calcium Carbonate: A Study of an Ascidian Skeleton*, Journal of the American Chemical Society 124, 32-39, 2002.

[41] http://csm.jmu.edu/minerals/CalciteKentucky.html; http://www.utexas.edu/tmm/npl/mineralogy/Blowups/Calcite_whiteVG19.htm; http://www.galleries.com/minerals/carbonat/calcite/calcite.htm; http://www.mineralsweb.com/s/77-Masterpiece-update/644-Cobaltoan-Calcite-SOLD/ (Accessed August 21st 2007).

[42] Weiner, S.; Addadi, L.; *Design strategies in mineralized biological materials*, Journal of Materials Chemistry 7, 689-702, 1997.

[43] http://www.magicalomaha.com/tumbledrocks.htm http://www.mineralium.com/index.php?lang=ENG&list=ART http://www.gc.maricopa.edu/earthsci/imagearchive/aragonite.htm (Accessed August 21st 2007).

[44] http://les.mineraux.free.fr/dossier-mineraux/minerauxrares/minerauxrares.htm http://www.mindat.org/show.php?id=4161&ld=2 (Accessed August 21st 2007).

[45] Falini, G.; Fermani, S.; Gazzano, M.; Ripamonti, A.; *Polymorphism and architectural crystal assembly of calcium carbonate in biologically inspired polymeric matrices*, Journal of the Chemical Society, Dalton Transactions 21, 3983-3987, 2000.

[46] Domingo, C.; Loste, E.; Gómez-Morales, J.; García-Carmona, J.; Fraile, J.; *Calcite precipitation by a high-pressure CO_2 carbonation route,* Journal of Supercritical Fluids 36, 202-215, 2006.

[47] Kitamura, M.; *Controlling factor of polymorphism in crystallization process,* Journal of Crystal Growth 237-239, 2205-2214, 2002.

[48] Kawano, J.; Shimobayashi, N.; Kitamura, M.; Shinoda, K.; Aikawa, N.; *Formation process of calcium carbonate from highly supersaturated solution*, Journal of Crystal Growth 237-239, 419-423, 2002.

[49] Kitamura, M.; Konno, H.; Yasui, A.; Masuoka, H.; *Controlling factors and mechanism of reactive crystallization of calcium carbonate polymorphs from calcium hydroxide suspensions*, Journal of Crystal Growth 236, 323-332, 2002.

[50] Donnet, M.; Bowen, P.; Jongen, N.; Lemaitre, J.; Hofmann, H.; *Use of Seeds to Control Precipitation of Calcium Carbonate and Determination of Seed Nature*, Langmuir 21, 100-108, 2005.

[51] Seo, K. S.; Han, C.; Wee, J. H.; Park, J. K.; Ahn, J. W.; *Synthesis of calcium carbonate in a pure ethanol and aqueous ethanol solution as the solvent*, Journal of Crystal Growth 276, 680-687, 2005.

[52] Yu, J.; Lei, M.; Cheng, B.; *Facile preparation of monodispersed calcium carbonate spherical particles via a simple precipitation reaction,* Materials Chemistry and Physics 88, 1-4, 2004.

[53] Mukkamala, S. B.; Anson, C. E.; Powell, A. K.; *Modelling calcium carbonate biomineralisation processes,* Journal of Inorganic Biochemistry 100, 1128-1138, 2006.

[54] Xiang, L.; Xiang, Y.; Wang, Z. G.; Jin, Y.; *Influence of chemical additives on the formation of super-fine calcium carbonate*, Powder Technology 126, 129-133, 2002.

[55] Chen, B. D.; Cilliers, J. J.; Davey, R. J.; Garside, J.; Woodburn, E. T.; *Templated Nucleation in a Dynamic Environment: Crystallization in Foam Lamellae*, Journal of the American Chemical Society 120, 1625-1626, 1998.

[56] Xiang, L.; Xiang, Y.; Wen, Y.; Wei, F.; *Formation of $CaCO_3$ nanoparticles in the presence of terpineol*, Materials Letters 58, 959-965, 2004.

[57] Kim, W. S.; Hirasawa, I.; Kim, W. S.; *Polymorphic Change of Calcium Carbonate during Reaction Crystallization in a Batch Reactor*, Industrial & Engineering Chemistry Research 43, 2650-2657, 2004.

[58] Söhnel, O.; Mullin, J. W.; *Precipitation of calcium carbonate,* Journal of Crystal Growth 60, 239-250, 1982.

[59] Morales, J. G.; Burgués, J. T.; Macipe, A. L.; Clemente, R. R.; *Precipitation of calcium carbonate from solutions with varying Ca^{2+}/carbonate ratios,* Journal of Crystal Growth 166, 1020-1026, 1996.

[60] Morales, J. G.; Burgués, J. T.; Clemente, R. R.; *Nucleation of calcium carbonate at different initial pH conditions*, Journal of Crystal Growth 169, 331-338, 1996.

[61] Pöykiö, R.; Nurmesniemi, H.; *Calcium carbonate waste from an integrated pulp and paper mill as a potential liming agent*, Environmental Chemistry Letters 6, 47-51, 2008.

[62] Japanese Laid-Open Patent Application No. Hei 10-226974.

[63] Konno, H.; Nanri, Y.; Kitamura, M.; *Crystallization of aragonite in the causticizing reaction,* Powder Technology 123, 33-39, 2002.

[64] Konno, H.; Nanri, Y.; Kitamura, M.; *Effect of NaOH on aragonite precipitation in batch and continuous crystallization in causticizing reaction,* Powder Technology 129, 15-21, 2003.

[65] Wang, C.; Xiao, P.; Zhao, J.; Zhao, X.; Liu, Y.; Wang, Z.; *Biomimetic synthesis of hydrophobic calcium carbonate nanoparticles via a carbonation route*, Powder Technology 170, 31-35, 2006.

[66] Gu, W.; Bousfield, D. W.; Tripp, C. P.; *Formation of calcium carbonate particles by direct contact of $Ca(OH)_2$ powders with supercritical CO_2*, Journal of Materials Chemistry 16, 3312-3317, 2006.

[67] Karagiozov, C.; Momchilova, D.; *Synthesis of nano-sized particles from metal carbonate by the method of reversed micelles*, Chemical Engineering and Processing 44, 115-119, 2005.

[68] Ono, Y.; *Catalysis in the production and reactions of dimethyl carbonate, an environmentally benign building block*, Applied Catalysis A: General 155, 133-166, 1997.

[69] Faatz, M.; Gröhn, F.; Wegner, G.; *Amorphous Calcium Carbonate: Synthesis and Potential Intermediate in Biomineralization*, Advanced Materials 16, 996-1000, 2004.

[70] Faatz, M.; Gröhn, F.; Wegner, G.; *Mineralization of calcium carbonate by controlled release of carbonate in aqueous solution,* Materials Science and Engineering C 25, 153-159, 2005.

[71] Faatz, M.; Cheng, W.; Wegner, G.; *Mechanical Strength of Amorphous $CaCO_3$ Colloidal Spheres*, Langmuir 21, 6666-6668, 2005.

[72] Guillemet, B.; Faatz, M.; Gröhn, F.; Wegner, G.; Gnanou, Y.; *Nanosized Amorphous Calcium Carbonate Stabilized by Poly(ethylene oxide)-b-poly(acrylic acid) Block Copolymers*, Langmuir 22, 1875-1879, 2006.

[73] Gorna, K.; Hund, M.; Vučak, M.; Gröhn, F.; Wegner, G.; *Amorphous calcium carbonate in form of spherical nanosized particles and its application as fillers for polymers*, Materials Science and Engineering A 477, 217-225, 2008.

[74] Chung, D.D.L.; *Composite Materials: Science and Applications,* Springer-Verlag: London, U.K., 2003.

[75] Milton, G.W.; *The Theory of Composites,* Cambridge University Press: Unitated Kingdom, 2002.

[76] Yu, L.; Dean, K.; Li, L.; *Polymer blends and composites from renewable resources,* Progress in Polymer Science 31, 576-602, 2006.

[77] Hull, D.; Clyne, T.W.; *An introduction to Composite Materials*, Cambridge University Press: 2nd Edition, Cambridge, U.K., 1996.

[78] Thostenson, E.T.; Li, C.; Chou, T.-W.; *Nanocomposites in context,* Composites Science and Technology 65, 491-515, 2005.

[79] Tjong, S.C.; *Structural and mechanical properties of polymer nanocomposites,* Materials Science and Engineering R 53, 73-197, 2006.

[80] Ray, S.; Easteal, A.J.; *Advances in Polymer-Filler Composites: Macro to Nano,* Materials and Manufacturing Processes 22, 741-749, 2007.

[81] Maeda, H.; Nakajima, M.; Hagiwara, T.; Sawaguchi, T.; Yano, S.; *Bacterial cellulose/silica hybrid fabricated by mimicking biocomposites*, Journal of Materials Science 41, 5646-5656, 2006.

[82] Matsumura, H.; Gugiyama, J.; Glasser, W. G.; *Cellulosic Nanocomposites. I. Thermally Deformable Cellulose Hexanoates from Heterogeneous Reaction*, Journal of Applied Polymer Science 78, 2242-2253, 2000.

[83] Matsumura, H.; Glasser, W. G.; *Cellulosic Nanocomposites. II. Studies by Atomic Force Microscopy,* Journal of Applied Polymer Science 78, 2254-2261, 2000.

[84] Nishino, T.; Matsuda, I.; Hirao, K.; *All-Cellulose Composite*, Macromolecules 37, 7683-7687, 2004.

[85] Nishino, T.; Arimoto, N.; *All-Cellulose Composite Prepared by Selective Dissolving of Fibre Surface*, Biomacromolecules 8, 2712-2716, 2007.

[86] Backfolk, K.; Lagerge, S.; Rosenholm, J. B.; Eklund, D.; *Aspects on the Interaction between Sodium Carboxymethylcellulose and calcium Carbonate and the Relationship to Specific Site Adsorption, ,* Journal of Colloid and Interface Science 248, 5-12, 2002.

[87] Bikiaris, D.; Panayiotou, C.; *LDPE/Starch Blends Compatibilized with PE-g-MA Copolymers,* Journal of Applied Polymer Science 70, 1503-1521, 1998.

[88] Bikiaris, D.; Prinos, J.; Koutsopoulos, K.; Vouroutzis, N.; Pavlidou, E.; Frangis, N.; Panayiotou, C.; *LDPE/plasticized starch blends containing PE-g-MA copolymer as compatibilizer,* Polymer degradation and Stability 59, 287-291, 1998.

[89] Stretenovic, A.; Müller, U.; Gindl, W.; *Mechanism of stress transfer in a single wood fibre-LDPE composite by means of electronic laser speckle interferometry*, Composites: Part A 37, 1406-1412, 2006.

[90] Hwang, C.; Hse, C.; Shupe, T. F.; *Effects of Recycled Materials on the Properties of Woodfiber-Polyethylene Composites. Part 2: Effect of a Compatibilizer on the Wettability of Birch Plywood and Polyolefins,* Forest Products Journal 57, 80-84, 2007.

[91] Krupa, I.; Chodák, I.; *Physical properties of thermoplastic/graphite composites,* European Polymer Journal 37, 2159-2168, 2001.

[92] Liu, X.; Husawake, H.; Kuwajima, S.; *Preparation of a PVdF-HFP/polyethylene composite gel electrolyte with shutdown function for lithium-ion secondary battery,* Journal of Power Sources 97-98, 661-663, 2001.

[93] Kamel, S.; Adel, A. M.; El-Sakhawy, M.; Nagieb, Z. A.; *Mechanical Properties and Water Absorption of Low-Density Polyethylene/Sawdust Composites,* Journal of Applied Polymer Science 107, 1337-1342, 2008.

[94] Lee, J.-H.; Jung, D.; Hong, C.-E.; Rhee, K. Y.; Advani, S. G.; *Properties of polyethylene-layered silicate nanocomposites prepared by melt intercalation with a PP-g-MA compatibilizer,* Composites Science and Technology 65, 1996-2002, 2005.

[95] Wang, M.; Joseph, R.; Bonfield, W.; *Hydroxyapatite-polyethylene composites for bone substitution: effects of ceramic particle size and morphology,* Biomaterials 19, 2357-2366, 1998.

[96] Yang, Y.-L.; G'Sell, C.; Hiver, J.-M.; Bai, S.-L.; *Dynamic Mechanical Properties and Morphology of High-Density Polyethylene/$CaCO_3$ Blends With and Without an Impact Modifier,* Journal of Applied Polymer Science 103, 3907-3914, 2007.

[97] Wang, W.-Y.; Zeng, X.-F.; Wang, G.-Q.; Chen, J.-F.; *Preparation and Characterization of Calcium Carbonate/Low-Density-Polyethylene Nanocomposites*, Journal of Applied Polymer Science 106, 1932-1938, 2007.

[98] Zhang, F.; Qiu, W.; Yang, L.; Endo, T.; Hirotsu, T.; *Mechanochemical preparation and properties of a cellulose-polyethylene composite*, Journal of Materials Chemistry 12, 24-26, 2002.

[99] Palaniyandi, V.; Simonsen, J.; *Effect of compatibilizers on the crystallization kinetics of cellulose-filled high density polyethylene,* Composite Interfaces 14, 73-83, 2007.

[100] Fendler, A.; Villanueva, M. P.; Gimenez, E.; *Characterization of the barrier properties of composites of HDPE and purified cellulose fibres*, Cellulose 14, 427-438, 2007.

[101] Wang, Q.; Chen, H.; Liu, Y.; *LDPE-g-MAH prepared through solid-phase mechanochemistry and its compatibilizing effects on HDPE/$CaCO_3$,* Polymer-Plastics Technology and Engineering 41, 215-228, 2002.

[102] T 237 om-93, *Carboxyl Content of Pulp*, TAPPI, 1993.

[103] Wunderlich, B.; *Macromolecular Physics*, volume 3, Academic Press, New York, 1980.

[104] Osman, M.A.; Atallah, A.; *Surfactant Chain Length and Tensile Properties of Calcium Carbonate-Polyethylene Composites*, Macromolecular Chemistry and Physics 208, 87-93, 2007.

[105] Parks, E.J.; Hebert, R.L.; *Thermal analysis of ion exchange reaction products of wood pulps with calcium and aluminum cations,* Tappi Journal 55, 1510-1514, 1972.

[106] Pascoal Neto, C.; Silvestre, A.J.D.; Evtuguin, D.V.; Freire, C.S.R.; Pinto, P.C.R.; Santiago, A.S.; Fardim, P.; Holmbom, B.; *Bulk and surface composition of ECF bleached hardwood kraft pulp fibres*, Nordic Pulp and Paper Research Journal 19, 513-520 , 2004.

[107] Xyla, A. G.; Koutsoukos, P. G.; *Quantitative Analysis of Calcium Carbonate Polymorphs by Infrared Spectroscopy*, Journal of Chemical Society, Faraday Transactions 1 85(10), 3165-3172, 1989.

[108] Gunasekaran, S.; Anbalagan, G.; *Spectroscopic characterization of natural calcite minerals,* Spectrochimica Acta Part A 68, 656-664, 2007.

[109] Rodriguez-Navarro, C.; Jimenez-Lopez, C.; Rodriguez-Navarro, A.; Gonzalez-Muñoz, M.T.; Rodriguez-Gallego, M.; *Bacterially mediated mineralization of vaterite,* Geochimica et Cosmochimica Acta 71, 1197-1213, 2007.

[110] Lee, H.S.; Ha, T.H.; Kim, K.; *Fabrication of unusually stable amorphous calcium carbonate in an ethanol medium,* Materials Chemistry and Physics 93, 376-382, 2005.

[111] Raz, S.; Testeniere, O.; Hecker, A.; Weiner, S.; Luquet, G.; *Stable Amorphous Calcium Carbonate Is the Main Component of the Calcium Storage Structures of the Crustacean Orchestis cavimana,* Biological Bulletin 203, 269-274, 2002.

[112] Fardim, P.; Durán, N.; *Modification of fibre surfaces during pulping and refining as analysed by SEM, XPS and ToF-SIMS*, Colloids and Surfaces A: Physicochemical and Engineering Aspects 223, 263-276, 2003.

[113] Freire, C. S. R.; Silvestre, A. J. D., Neto, C. P.; Gandini, A.; Fardim, P.; Holmbom, B.; *Surface characterization by XPS, contact angle measurements and ToF-SIMS of cellulose fibres partially esterified with fatty acids,* Journal of Colloid and Interface Science 301, 205-209, 2006.

[114] Fardim, P.; Gustafsson, J.; Shoultz, S.; Peltonen, J.; Holmbom, B.; *Extractives on fiber surfaces investigated by XPS, ToF-SIMS and AFM,* Colloids and Surfaces A: Physicochemical and Engineering Aspects 255, 91-103, 2005.

[115] Gullichsen, J.; Paulapuro, H.; *Papermaking Science and Technology: Forest Products Chemistry*, Book 3, Fapet Oy: Finland, 2000.

[116] Kroschwitz, J.I.; *Polymers: Polymer Characterization and Analysis*, John Wiley & Sons: U.S.A., 1990.

[117] Zhang, S.; Gonsalves, K. E.; *Influence of the Chitosan Surface Profile on the Nucleation and Growth of Calcium Carbonate Films*, Langmuir 14, 6761-6766, 1998.

[118] Matsushita, I.; Suzuki, T.; Moriga, T.; Ashida, T.; *XPS Study on the Carbonation Process of $Ca(OH)_2$,* Journal of the Ceramic Society of Japan 101, 725-727, 1993.

Gopinath, C. S.; Hedge, S. G.; Ramaswamy, A. V.; Mahapatra, S.; *Photoemission studies of polymorphic $CaCO_3$ materials,* Materials Research Bulletin 37, 1323-1332, 2002.

Wu, W.; He, T.; Chen, J.-f.; Zhang, X.; Chen, Y.; *Study on in situ preparation of nano calcium carbonate/PMMA composite particles*, Materials Letters 60, 2410-2415, 2006.

[119] Shui, M.; *Polymer surface modification and characterization of particulate calcium carbonate fillers,* Applied Surface Science 220, 359-366, 2003.

[120] http://www.casaxps.com/help_manual/XPSInformation/IntroductiontoXPS.htm (Accessed May 6th 2008).

[121] Benelux Scientific Case study; *Characterization of PE with DSC and DMA*, Netzch Applications Laboratory Newsletter, 09-2005-03, http://www.benelux-scientific.com/foto/netzch-09-2005-03.pdf (Accessed March 11th 2008).

[122] Gmelin, E.; Sarge, S.M.; *Temperature, heat and heat flow rate calibration of differential scanning calorimeters,* Thermochimica Acta 347, 9-13, 2000.

[123] Gupta, B.; Revagade, N.; Hilborn, J.; *Poly(lactic acid) fiber: An overview,* Progress in Polymer Science 32, 455-482, 2007.

[124] Oksman, K.; Skrifvars, M.; Selin, J.-F.; *Natural fibres as reinforcement in polylactic acid (PLA) composites,* Composites Science and Technology 63, 1317-1324, 2003.

Mathew, A. P.; Oksman, K.; Sain, M.; *Mechanical Properties of Biodegradable Composites from Poly Lactic Acid (PLA) and Microcrystalline Cellulose (MCC),* Journal of Applied Polymer Science 97, 2014-2025, 2005.

Mathew, A. P.; Oksman, K.; Sain, M.; *The Effect of Morphology and Chemical Characteristics of Cellulose Reinforcements on the Crystallinity of Polylactic Acid,* Journal of Applied Polymer Science 101, 300-310, 2006.

Kasuga, T.; Maeda, H.; Kato, K.; Nogami, M.; Hata, K.; Ueda, M.; *Preparation of poly(lactic acid) composites containing calcium carbonate (vaterite)*, Biomaterials 24, 3247-3253, 2003.

Maeda, H.; Kasuga, T.; *Preparation of poly(lactic acid) composite hollow spheres containing calcium carbonates*, Acta Biomaterialia 2, 403-408, 2006.